# EFFECTS OF POROUS ROTATING FRAME ON PERISTALTIC MHD JEFFREY FLUID FLOW

**By**

**Ayesha Akhtar**


**NATIONAL UNIVERSITY OF MODERN LANGUAGES**
**ISLAMABAD**

**December, 2025**

# EFFECTS OF POROUS ROTATING FRAME ON PERISTALTIC MHD JEFFREY FLUID FLOW

**By**
**Ayesha Akhtar**

MS MATH'S, NATIONAL UNIVERSITY OF MODERN LANGUAGES ISLAMABAD
2025 A THESIS SUBMITTED IN PARTIAL FULFILMENT OF
THE REQUIREMENTS FOR THE DEGREE OF

**MASTER OF SCIENCE**
**In MATHEMATICS**

TO
FACULTY OF ENGINEERING AND COMPUTING


NATIONAL UNIVERSITY OF MODERN LANGUAGES ISLAMABAD


# THESIS AND DEFENSE APPROVAL FORM

**The undersigned certify that they have read the following thesis, examined the defense, are satisfied with overall exam performance, and recommend the thesis to the Faculty of Engineering and Computing for acceptance.**

**Thesis Title:** Effects of Porous Rotating Frame on Peristaltic MHD Jeffrey Fluid Flow

**Submitted By:** Ayesha Akhtar **Registration #:** 95 MS/Math/F23

Master of Science in Mathematics
Title of the Degree

Mathematics
Name of Discipline

Dr. Hadia Tariq
Name of Research Supervisor

Signature of Research Supervisor

Dr. Anum Naseem
Name of HOD

Signature of HOD

Dr. Noman Malik
Name of Dean (FEC)

Signature of Dean (FEC)

December 16, 2025

# AUTHOR'S DECLARATION

I Ayesha Akhtar

Daughter of Akhtar

Registration # 95 MS/Math/F23

Discipline Mathematics

Candidate of **Master of Science in Mathematics (MS MATH)** at the National University of Modern Languages do hereby declare that the thesis **Effects of Porous Rotating Frame on Peristaltic MHD Jeffrey Fluid Flow** submitted by me in partial fulfillment of MS Math degree, is my original work, and has not been submitted or published earlier. I also solemnly declare that it shall not, in future, be submitted by me for obtaining any other degree from this or any other university or institution. I also understand that if evidence of plagiarism is found in my thesis/dissertation at any stage, even after the award of a degree, the work may be cancelled and the degree revoked.

_____
Signature of Candidate

Ayesha Akhtar
Name of Candidate

16th December, 2025
Date

# ABSTRACT

**Title: Effects of Porous Rotating Frame on Peristaltic MHD Jeffrey Fluid Flow**

This study focuses on the peristaltic transport of a Jeffrey fluid within a porous rotating frame under the influence of magnetohydrodynamics (MHD). The Jeffrey fluid model, which accounts for relaxation and retardation times is considered to better describe the viscoelastic characteristics of biological and industrial fluids. The governing equations describing the system are non-linear and non-homogeneous partial differential equations formulated in Cartesian coordinates. By applying the lubrication approximation, assuming a low Reynolds number and long wavelength, the momentum equations are simplified and solved using the perturbation method. Analytical solutions are obtained and further examined through symbolic computation using Mathematica.

The novelty of this research lies in addressing the unexplored effects of rotation on Jeffrey fluid peristaltic flow in a porous medium under MHD conditions, an area that has received limited attention in the literature. The study investigates how the velocity distribution and streamline patterns are influenced by variations in rotational and magnetic parameters. The outcomes are expected to provide deeper insights into the behavior of non-Newtonian fluids in rotating porous environments, with potential applications in biomedical devices, polymer processing, and peristaltic pumping technologies widely used in industry.

# TABLE OF CONTENTS

# LIST OF FIGURES

# LIST OF SYMBOLS

| | |
|---|---|
| $\epsilon$ | Sutterby fluid parameter |
| $\delta$ | Dimensionless wave number |
| $Ec$ | Eckert number |
| $Da$ | porosity parameter |
| $Re$ | Reynolds number |
| $Hc$ | Heat source parameter |
| $Me$ | Magnetic parameter |
| $\theta$ | Dimensionless temperature |
| φ | Amplitude ratio |
| $Pr$ | Prandtl number |
| $\Omega$ | Rotation parameter |
| $Q_0, Q_1$ | Flow rate |
| $\rho$ | Density |
| $P$ | Pressure |
| μ | Dynamic viscosity |
| $\nu$ | Kinematic viscosity |
| $C_p$ | Specific Heat |

| | |
|---|---|
| $\boldsymbol{k}$ | Thermal Conductivity |
| $\boldsymbol{s}$ | Wave propagation speed |
| $\boldsymbol{\omega}$ | Wavelength |
| $\boldsymbol{\varphi}^{*}$ | Amplitude of a peristaltic wave |
| $\boldsymbol{d^{*}}$ | Average radius of the tube |

# ACKNOWLEDGMENT

I want to thank and honor Allah Ta'ala for making this study possible and fruitful. Without the sincere support provided by numerous sources for which I would want to sincerely thank you this project could not have been completed. However, a lot of people helped me succeed, and I will always be grateful for their support. I owe a debt of gratitude to Dr. Hadia Tariq, whose counsel, insight, and steadfast support have been invaluable to me during this study process. I consider myself extremely fortunate to have had her as my mentor because her knowledge and guidance have been helpful.

# DEDICATION

*This thesis work is dedicated to my parents and my teachers, whose steadfast encouragement and support have propelled me to pursue my academic goals. I am incredibly appreciative to my parents for their traits and contributions that have inspired and pushed me during this journey. Your advice and kindness have been a consistent source of support.*

# CHAPTER 1

# INTRODUCTION AND LITERATURE REVIEW

## 1.1 Introduction

The study of fluid mechanics focuses on comprehending and controlling the fluid's behavior. Fluid mechanics is a significant area of the applied sciences with a wide range of fascinating and useful applications for engineers. A basic understanding of fluid mechanics is essential to daily living because we inhabit a planet primarily covered by liquid with a dense gas environment. There is an immense dependence on fluid machinery in our surroundings. Pumps, steam turbines, sewage, electrical systems, airplanes, cars, ships, spacecraft, and almost every other vehicle interact with fluid of some kind, either as part of an engine or as a hydraulic control system. Gaining knowledge of fluid mechanics also helps us comprehend our body and a variety of fascinating aspects of our surroundings. For instance, the heart and lungs are perfectly made pumps that function sporadically. However, the lungs efficiently cycle air through the branching pulmonary passages, and the heart efficiently pumps blood through the branching network of arteries, capillaries, and veins.

Fluid dynamics and fluid statics have historically been the two subfields of fluid mechanics. The behavior of a fluid at rest or almost at rest is the focus of fluid statics, often known as hydrostatics and fluid dynamics is the field that studies fluids in motion.

Several characteristics, such as viscosity, density, temperature, specific heat, pressure, and thermal conductivity, are used to categorize fluids into different types. Fluid viscosity has significant impact on fluid flow. The fluid having constant viscosity is the type of fluid called Newtonian fluids (Bansal, 2004). Example includes most common fluids water and air. Non-Newtonian fluids play an important role in physiological and industrial processes because of their unique and adjustable flow characteristics. Newton's law of viscosity, which specifies that a fluid's viscosity remains constant irrespective of applied stress, is not followed by these fluids. Rather, a non-Newtonian fluid is the one whose thickness or viscosity, varies in response to applied force. A wide range of naturally occurring materials, such as paints, ketchup, blood and shampoo display

non-Newtonian behavior.

## 1.2 Peristalsis

Peristalsis is the process of contraction and relaxation of the surrounding flexible muscles or structures to facilitates the movement of material. Such processes include, for instance, the swallowing of food, the motion of digested food in the intestine, the flow of urine to the bladder, blood circulation in heart as well as in lungs, etc.

Complex and profound nature of the fluid's peristaltic motion within a conduit while experiencing a magnetic field, has attracted much attention in a number of studies. Engineers find peristaltic pumping particularly appealing because it leverages natural mechanisms to reduce work piece handling and provides stability in practical applications. The study about peristalsis was first presented by (Latham, 1966). This study served as the milestone to study Newtonian and non-Newtonian fluids flowing past the tubes or channels exhibiting peristaltic mechanism.

(Burns & Parkes, 1967) examined the flow of a viscous fluid via symmetrical channel and axially symmetric pipe, assuming that the Reynolds number is low enough to allow for the utilization of Stokes flow approximations. It was assumed that the pipe or channel's cross-section fluctuates sinusoidally over its length. (Barton & Raynor, 1968) studied the flow of peristaltic fluid in tubes, two flow domains of peristaltic motion in tubes had been investigated in this article. The wall disturbance wavelength in the first analysis was significantly greater than the average tube radius. The wall disturbance wavelength in the second analysis was smaller as the average radius. In a study by (Brown & Hung, 1977) , both computational and experimental approaches had been used to investigate two-dimensional nonlinear peristaltic flows. The Navier-Stokes equations for peristaltic flows with finite Reynolds number and wall-wave curvature were solved implicitly using a finite-difference method with orthogonal curvilinear coordinates.

(Böhme & Friedrich, 1983) used an infinite train of sinusoidal waves traveling down the duct wall to study the peristaltic movement of an incompressible viscoelastic fluid in the case of a plane flow. The main assumptions were that the relevant Reynolds number was sufficiently small to ignore inertia effects and that the wavelength to channel height ratio is large, indicating that the pressure was constant across the cross-section.

Both Newtonian and non-Newtonian nanofluid peristaltic flow in a uniform and non-uniform tube channel was investigated by (Shaheen, 2017). The research illustrated the impact of multiple factors on nanofluid's flow caused by pressure gradient involving endoscopic tubes, convective boundary conditions, magnetic fields and viscous dissipation.

(Fauci, 1992) studied the peristalsis pumping of solid particle. This work used sinusoidal waves to simulate the peristalsis-based solid particle transport in a two-dimensional channel. The particle and the channel walls were considered to be neutrally buoyant elastic barriers submerged in a viscous, incompressible fluid. The absorbed boundary technique allowed them to computationally model fluid particle interaction. (Kumar & Naidu, 1995) conducted a numerical analysis of peristaltic flows. For two-dimensional peristaltic flow, the Navier-Stokes equations in $\Psi - \omega$ form were numerically solved. For flow analysis, an easy nonlinear streamline quadrature upwinding noniterative $\Psi - \omega$ finite element approach was used. For different peristaltic flows, the velocity, stress fields and pressure were identified. The outcomes were contrasted with those of finite difference analysis and perturbation analysis.

The problem of the peristaltic movement of a viscous incompressible fluid in a porous media in an asymmetric channel was examined by (Elshehawey *et al*., 2006). The peristaltic flow of a Newtonian fluid which was incompressible through a porous medium in an asymmetric channel was examined in this work. The flow was studied in a wave frame of reference moving with the wave's velocity, assuming a long wavelength and a low Reynolds number. The effects of heat transfer and a magnetic field on the peristaltic motion of a viscous incompressible Newtonian fluid via porous medium in a vertical tube were examined by (Vasudev *et al*., 2011), assuming a long wavelength and a low Reynolds number.

Peristaltically flowing Non-Newtonian and Newtonian fluids under various conditions has been the subject of numerous studies. (Hayat & Ali, 2008) investigated the peristaltic motion of a Jeffrey fluid in a tube with sinusoidal waves traveling down its wall. The fluid was electrically conducting when a uniform magnetic field was present. A study by (Nadeem & Akbar, 2009) was carried out to explain how heat transfer affects the Herschel-Bulkley fluid's peristaltic movement in a nonuniform inclined tube. A Williamson model's peristaltic flow in an asymmetric channel was demonstrated by (Nadeem & Akram, 2010), its governing equation for two-dimensional peristaltic flow phenomena were built using long wave length and low Reynolds numbers approximations. A study on the peristaltic flow of a Carreau fluid in a rectangular duct was carried out by (Nadeem

*et al.*, 2012). They examined the flow in the wave frame of reference leaving the fixed frame with velocity. The peristaltic wave propagating on a rectangular duct's horizontal side walls under long wave length and low Reynolds number approximation was studied.

## 1.3 Porous Medium

In recent years, there has been significant interest among geophysical fluid dynamists in studying flow through porous media. A material that has a network of linked pores within it that allow liquid to flow through or around them is called a porous medium. Darcy's law by (Scheidegger, 1957), which describes the fluid's passage within porous medium, has been employed in number of publications. Numerous spatial characteristics, such as permeability, porosity, hardness, and others, are able to differentiate between different types of porous media. However, the two most prominent qualities among them are porosity and permeability, (Jawad & Abdulhadi, 2023). Porous media can contain an extensive variety of materials, including biological tissues like wood and bone, natural substances like rocks, and man-made materials like cement. Numerous scientific and engineering fields, such as petroleum engineering, earth sciences, construction engineering, petroleum geology, materials science and geophysics use porous media extensively. Friction among the walls of the medium and liquid causes the fluid to flow through porous media, obstructing the fluid's passage (Jawad & Abdulhadi, 2023).

A research was carried out by (Sochi, 2010) to cover the single-phase flow of non-Newtonian fluids in porous media. In this context, the four primary methods for characterizing the flow through porous media in general were analyzed and evaluated including pore-scale network modelling, numerical techniques, continuum models, and bundle of tubes models.

Heat transfer researchers are constantly looking for new methods to enhance heat transfer and maximize the performance of energy devices. The simultaneous used of nanofluids and porous media for improving heat transfer in thermal systems with multiple structures, flow regimes, and boundary conditions is thoroughly reviewed in a research by (Kasaeian *et al*., 2017).

(Eldesoky *et al*., 2020) examined how a compressible Maxwell fluid with MHD was affected by both wall characteristics and space porosity. In this study, a fixed magnetic field is provided to an axisymmetric tube with a solid wall to evaluate the peristaltic motion of a viscous Maxwell fluid

as it flows through a porous media. (Javid *et al.*, 2022) investigated the impact of porosity on the peristaltic motion of biological fluid in a complicated curvy channel. This work considered biological fluid's steady, laminar rheology from a biomimetic conduit. The non-Newtonian parameters and porosity were two embedded parameters that regulate the rheology. The MHD peristaltic flow of a non-Newtonian fluid across a tapered asymmetric channel was the focus of a study by (Vaidya *et al*., 2020). A porous medium is used to carry fluids having varying transport qualities, such as viscosity and thermal conductivity.

(Nallapu & Radhakrishnamacharya, 2014) studied Jeffrey fluid flow through porous media in tubes with small diameters when a magnetic field was present. The investigation of the peristaltic motion of a Jeffrey fluid in a tube through a porous medium with sinusoidal waves traveling along its wall under the influence of rotation and a magnetic field is the focus of study by (Mahmoud, 2011). (Ellahi *et al*., 2014) studied the effects of MHD on the Jeffrey fluid's peristaltic flow in a rectangular conduit through a porous medium. Under the effect of rotating frame with a chemical reaction, another work by (Abd-Alla, Abo-Dahab, Thabet, *et al*., 2023) offered a basic understanding of how mass and heat transfer affect the MHD Jeffrey fluid peristaltic flow occupying porous space in a symmetric inclined channel.

## 1.4 Magnetohydrodynamics (MHD)

A number of studies investigated how a magnetic field effects fluid flow. A magnetic field produced by electric current has an immense impact on fluid's flow within a channel. Many researchers have been inspired by this aspect to investigate its applications across various scientific domains, such as the separation devices, MHD energy generators, MHD medication targeting, cancer treatment, materials processing, magnetofluid rotary blood pumping and health sciences. Researchers use MHD to investigate the wide range of conditions with applications ranging from biomedical applications to space exploration.

(Abbas & Hayat, 2008) examined the impacts of radiation on the magnetohydrodynamics (MHD) flow of an incompressible viscous fluid in a porous media, a non-linear stretched sheet induces the flow. An electrically conducting fluid's steady MHD asymmetric flow past a semi-infinite stationary plate was examined in a study when radiation was present, also the impact of the radiation parameter was examined, and numerical solutions for the temperature field had been obtained (Raptis, Perdikis, & Takhar, 2004). (Khan & Rafaqat, 2021) examined the effects of

MHD and radiation on compressible Jeffrey fluid with peristalsis. This research examined the MHD effect on compressible fluids as well as heat transmission via thermal radiation. It had been discussed how surface acoustic waves at the microchannel's edges can induce peristalsis.

The study by (Al-Khafajy, Lelo, & Shallal, 2021) investigated how change in viscosity effect mass transfer in MHD oscillatory flow with in porous medium using Carreau fluid. The fluid in which the viscosity changes with different temperature is Carreau fluid. In a study by (Reddy & Reddy, 2015), they described the impact of MHD along with the Joule heating effects on nanofluid flowing past a tube with peristaltic waves induced. (Reddy, 2016) investigated the heat and mass transfer of the fluid flow in a porous channel with the slip effects at the boundaries. This study concluded that the velocity of the fluid dropped by enhancing the magnetic paramtere while increaded with the increase in the porosity. (Hayat *et al.*, 2018) studied the two-phase non-Newtonian fluid flow with MHD induced flowing past an annulus. It was observed that the velocity dropped at the midpoint of the channel with the rise in the magnetic parameter while a surge in the velocity was noted at the boundaries. To study the impact of MHD on the Newtonian fluid, (Srinivas & Kothandapani, 2009) investigated the fluid flow in a flexible channel with porous medium. Using MHD, heat transfer analysis and nonlinear slip effects, (Ellahi & Hameed, 2012) conducted a numerical analysis of steady non-Newtonian flows.

(Ali *et al*., 2023) examined the MHD influence on the peristaltic Casson fluid along with slip conditions at the boundaries. In a study conducted by (Hafez, Abd-Alla, & Metwaly, 2023), the impact of heat and mass transfer on the hydro-magnetic peristaltic flow of a Casson fluid via an asymmetric channel in a rotating inclined system was examined. Recently a study by (Gudekote *et al.*, 2024) investigated how magnetohydrodynamics effects the Eyring-Powell fluid's peristaltic motion. This study looked into how wall properties affect peristalsis when a magnetic field was present and also considered variable liquid properties like changing viscosity and thermal conductivity.

The MHD flow of a non-Newtonian fluid on a porous plate is the subject of the research by (Hafez, Abd-Alla, & Metwaly, 2023). It had been analyzed that an electrically conducting second order incompressible fluid surrounded by an infinite non-conducting porous plate and subjected to a uniform suction or blowing has two perfect solutions for non-torsional induced unsteady hydro-magnetic flow.

## 1.5 Jeffrey Fluid

Among many non-Newtonian fluid models, Jeffrey fluid model have caught the attention from researchers. (Hayat *et al.*, 2006) emphasized that it provides more accurate description of physiological fluids. A more basic linear model of viscoelastic fluid is the Jeffrey fluid. The only model that is capable of accurately depict the stress relaxation property is the Jeffrey fluid model. It has been determined that the Jeffrey fluid is an extension of standard Newtonian fluid as its constitutive equation can be simplified to that of the Newtonian model as a specific case. Unique memory time scale, commonly referred to as the relaxation time is a characteristic of Jeffrey fluid model which provides a great description of a class of non-Newtonian fluids.

The Jeffrey fluid holds significant in various research fields and industries where viscoelastic material are used such as food rheology, biomedical applications and polymer processing. Fluid flow including that of certain polymers and biological fluids, can be described by it.

Jeffrey fluid have been researched in a variety of circumstances by numerous researchers. The effect of MHD on a Jeffrey fluid was included in a detailed investigation by AL-Khafajy (Salih, 2020), in which peristaltic flow through slanted porous channel in a cylindrical polar coordinate system was investigated. (Vajravelu, Sreenadh, & Lakshminarayana, 2011) investigated how heat transmission effects Jeffrey fluid's peristaltic flow. (Jyothi, Devaki, & Sreenadh, 2013) looked into the Jeffrey fluid's pulsatile motion in a circular tube with an inner porous medium lining. Research had been done on the peristaltic motion of a Jeffrey fluid model within an asymmetric channel in the existence of magnetic field by (Kothandapani & Srinivas, 2008) and (Pandey & Tripathi, 2010). (Nallapu & Radhakrishnamacharya, 2015) studied a two-fluid model for the passage of Jeffrey fluid across a porous medium in tubes having small diameters.

In a recent study, impact of heat transfer and magnetic field on Jeffrey fluid's peristaltic motion with in porous medium in an asymmetric channel is investigated by (Abd-Alla, Abo-Dahab, Salah, et al., 2023). Peristaltic motion of Jeffrey fluid through a duct with an elliptic cross-section was analytically explored by (Nadeem *et al*., 2023) to figure out the interpretation of heat and mass transfer. A study by (Rafiq *et al.*, 2022) was carried out to study the peristaltic motion of Jeffrey nanofluid in the existence of magnetic field within tapered asymmetric channel. The main objective of this study was to examine the heat transmission property of nanofluid in order to treat different diseases including cancer. Another study by (Farooq *et al*., 2023) was carried out to study

the Jeffrey fluid's peristaltic motion that conducts electricity. The walls within the peristaltic propagation channel were inclined and asymmetric. Applying a transverse magnetic field to the flow takes into consideration the effects of joule heating and magnetic field.

## 1.6 Rotational Effect

Many studies have been conducted on non-Newtonian fluids peristaltically flowing under the effect of rotation. (Nouri & Whitelaw, 1997) examined the Newtonian and non-Newtonian fluid's flow in an eccentric annulus as the inner cylinder rotates. With a more consistent axial flow across the annulus and the highest tangential velocities in the tightest gap in both situations, the results demonstrated that the rotation had similar impacts on the Newtonian and non-Newtonian fluids. The flow and heat transmission of upper-convected Maxwell (UCM) fluid in a rotating frame were investigated analytically in study by (Mustafa, Hayat, & Alsaedi, 2017). Consideration was given to fluids whose thermal conductivity varies with temperature. The heat transfer process is modelled using a non-Fourier heat flux term that incorporates thermal relaxation effects.

(Ayub, Ahmad, & Ahmad, 2022) discussed MHD rotating flow of a viscous fluid through porous media by means of a vertical plate with slip and hall effect. Therefore, the objective of this paper was to shed light on slip effect over the rotational flow and free convection of a viscous fluid over an extended plate with heat and mass transfer when a constant magnetic field is present with in porous medium. Since the fluid in discussion was chemically reacting, the construction of governing equations takes into account the impact of both chemical reaction and heat absorption.A study by (Mohammed & Hummady, 2023) looked how rotation impacts Sutterby fluid's peristaltic flow in an asymmetric channel exhibiting heat transmission. Another research by (Moeana & Al-Khafajy, 2024) examined the temperature and rotation-influenced MHD peristaltic flow of Sutterby fluid within a porous medium. Effects of fluid viscosity, average tube radius, rotation, and magnetic field on fluid movement and temperature have all been examined in this work.

## 1.7 Thesis Contribution

This thesis provide an in-depth examination of the work done by (Moeana & Al-Khafajy, 2024). They looked into the impact of rotation on the temperature and MHD peristaltically flowing non-Newtonian Sutterby fluid through porous wave medium. This work has been extended considering

Jeffrey fluid model instead of Sutterby fluid model and investigates how rotation effects the temperature and MHD peristaltic flow of a non-Newtonian Jeffrey fluid through porous medium. The momentum equation has been solved using perturbation approach while considering long wavelength and low Reynolds number. At the end graphs are generated using program "Mathematica 13" for different components.

## 1.8 Thesis Organization

Thesis is further divided into following chapters. The clear overview of chapters is as follows:

**Chapter 1** provides in-depth overview of literature and it is thoroughly reviewed in accordance with recently released publications.

**Chapter 2** offers the fundamental concepts, principles and dimensionless parameters in order to acquire numerical solution and result for the flow problem.

**Chapter 3** reviews the work of (Moeana & Al-Khafajy, 2024) which examines the effects of rotation on the temperature and MHD peristaltically flowing non- Newtonian Sutterby fluid through porous wave medium.

**Chapter 4** extends the review work by examining how rotation influences peristaltic MHD Jeffrey fluid flow through porous media.

**Chapter 5** includes conclusion obtained by the overall study and recommendations for further research.

The list of all references utilized in this research work are provided at the end.

# CHAPTER 2

# BASIC CONCEPTS AND DEFINITIONS

## 2.1 Fluid Mechanics

The analysis of fluid behavior in motion or at rest is the focus of the physical science field of fluid mechanics. Statics and dynamics are the two subfields of the fluid mechanics, which further subdivide into compressible and incompressible flow. There are two types of incompressible and compressible flow: ideal and real. Real split into turbulent and laminar flow. Following five physics principles form the foundation of fluid mechanism, (Granger, 2012).

- Mass conservation
- Energy Conservation
- Linear momentum conservation
- Angular momentum conservation
- Second law of thermodynamics

Fluid mechanics has undeniable scientific significance since the atmosphere and oceans that cover this planet are fluids, and the great bulk of the observable mass in the universe resides in a fluid state. The practical significance of fluid mechanics is likewise undeniable, since it is the fundamental field for transportation systems, power generation and converters, material processing and manufacturing, food production, and civil infrastructure. Like any other area of the physical sciences, advances in fluid mechanics can result from experiments, computer stimulation, or mathematical studies. Analytical methods are frequently effective in solving idealized and simplified problems, and these solutions can be extremely valuable for acquiring understanding and insight as well as for comparison with experimental and numerical data (Kundu *et al*., 2024).

## 2.2 Fluids

Any substance that has the ability to flow is considered fluid. Fluid is defined as any substance that constantly deforms when exposed to even a slight shear force. Because of their constant volume, liquids cannot fill a big container fully; instead, a free surface isolates the liquid from its vapor in a gravitational field. They have strong cohesive forces. However, with a specified volume and few cohesive forces, gas always expands and fills the entire container (Kundu *et al.*, 2024).

## 2.3 Properties of Fluids

Fluid can be classified into several categories and show different behaviors based on different properties including density, viscosity, temperature, specific heat, thermal conductivity, pressure and surface tension etc.

### 2.3.1 Dimension and Units

The temperature $[\theta]$, length $[L]$, mass $[M]$ and time $[T]$ are key dimensions in fluid mechanics. The units are kelvin for temperature, meter for length, second for time and kilogram for mass. In fluid mechanics, they are the fundamental units from which all physical quantities can be obtained. The table 2.1 lists a few common physical quantities together with their SI units and symbols (Kundu *et al.*, 2024).

**Table 2.1** Physical Quantities

| Quantity | Name of unit | Symbol | Equivalent |
|---|---|---|---|
| Length | Meter | m | |
| Mass | Kilogram | kg | |
| Time | Second | s | |
| Temperature | Kelvin | K | |
| Frequency | Hertz | Hz | $s^{-1}$ |
| Force | Newton | N | $kg\ ms^{-2}$ |
| Pressure | Pascal | Pa | $N\ m^{-2}$ |
| Energy | Joule | J | $N\ m$ |
| Power | Watt | W | $J\ s^{-1}$ |

### 2.3.2 Density

Density is the measure of mass per volume. It is ratio of the mass of fluid to the volume that a material occupies. $\rho$ symbol is used to denote density.

Mathematically,

$$\rho = \frac{mass\ of\ fluid}{volume}.$$

SI unit of density is $\frac{kg}{m^3}$ (Bansal, 2004).

### 2.3.3 Pressure

When a fluid is at rest, its normal stress is called pressure it is presumed to be positive in compressive fluids, (Granger, 2012). It is the force per unit area denoted by *P*.

Mathematically,

$$P = \frac{Force}{Area}.$$

$\frac{N}{m^2}$ is the SI unit of pressure.

### 2.3.4 Viscosity

The property of a fluid which causes resistance to its movement is called viscosity. Kinematic and dynamic viscosity are the two types into which viscosity is classified.

Dynamic viscosity is defined as when one fluid layer resists to flow across another adjacent fluid layer. SI unit of dynamic viscosity is $\frac{Ns}{m^2}$ and μ (mu) is the coefficient of dynamic viscosity.

Kinematic viscosity is referred to as dynamic viscosity divided by its density. $\frac{m^2}{s}$ is the SI unit of kinematic viscosity and it is denoted by $\nu$ (Bansal, 2004).

### 2.3.5 Specific Heat

The quantity of heat energy needed to rise the temperature of fluid of a unit mass by unit degree is known as the specific heat capacity $C_p$. Temperature and the method of adding heat both effect the value of $C_p$ (Shaughnessy, Katz, & Schaffer, 2005).

### 2.3.6 Thermal Conductivity

A substance's capacity to conduct heat or its ability to allow flow of heat under temperature gradients is calculated by its thermal conductivity. It is denoted by the letter $k$.

$$k = \frac{QL}{A\Delta T},$$

here, Q represents heat flow per unit time, $\Delta T$ is change in temperature and and $A$ refers to cross sectional area.

## 2.4 Types of Fluid

The fluids can be further grouped into ideal, real, ideal plastic, Newtonian and non-Newtonian fluids. (Bansal, 2004)

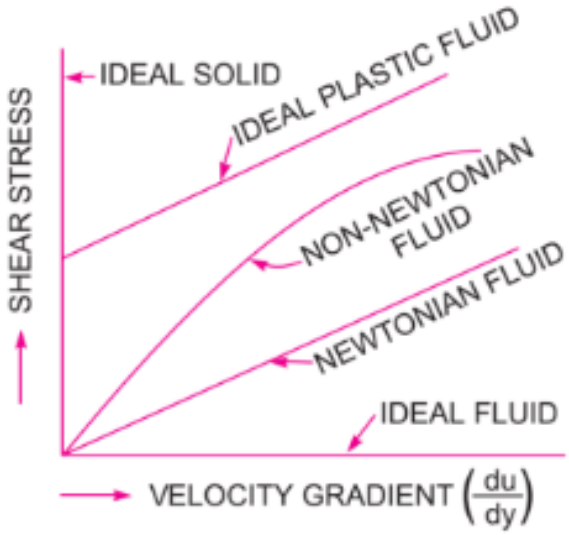


**Figure 2.1** Fluid Types

### 2.4.1 Ideal Fluids

Ideal fluids are also known as perfect fluids, they have zero viscosity and constant density. It is referred to an imaginary fluid since every fluid in existence has some viscosity (Bansal, 2004).

### 2.4.2 Real Fluids

A real fluid is defined as one that has viscosity. As a matter of fact, every fluid that exists is a real fluid (Bansal, 2004).

### 2.4.3 Ideal Plastic Fluids

When shear stress surpasses the yield stress value and is directly proportional to the rate of shear strain then this type of fluid is called as ideal plastic fluids (Bansal, 2004).

### 2.4.4 Newtonian Fluids

A Newtonian fluid is referred to as a fluid that conforms with Newton's law of viscosity. It emphasizes that rate of shear stress and shear strain are directly proportional (Bansal, 2004).

### 2.4.5 Non-Newtonian Fluids

A type of fluid where the rate of shear strain and shear stress are not directly proportional. It doesn’t conforms with Newton’s law of viscosity (Bansal, 2004).

## 2.5 Flow

In fluid mechanics, flow is defined as the fluid’s motion. It is very important to understand fluid flow in order to understand fluids behavior as well as their interaction with surroundings.

Following are the different kinds of fluid flow.

### 2.5.1 Unsteady Flow and Steady Flow

In a steady flow, the fluid's density, pressure, and velocity do not change over time, they remain constant. However, in unsteady flow the properties like density, pressure and velocity are vary with time (Bansal, 2004).

### 2.5.2 Laminar Flow and Turbulent Flow

A laminar flow is one having all the stream lines parallel and straight, and particles of fluid flow along well specified paths or stream lines. So, the particles float easily upon the succeeding layer as they move in laminas or layers (Bansal, 2004). Because adjacent layers glide past one another smoothly and the fluid often flows without lateral mixing al low velocity, it typically occurs in small viscous pipes with low fluid velocity. There are no fluid swirls or eddies in laminar flow.

The movement of fluid particles in a zig zag pattern is known as turbulence or turbulent flow. The eddies that occur as a result of the particles moving in a zig zag pattern are responsible for the significant energy loss. Randomness is one of the characteristics of turbulent flow, which makes flows seem erratic, unpredictable and chaotic. Nonlinearity, heat and momentum diffusion, and a high degree of fluctuating vorticity are also included (Kundu *et al.*, 2024).

### 2.5.3 Uniform Flow and Non-Uniform Flow

The uniform flow is described as a flow type having constant velocity relative to space. Conversely, a non-uniform flow is one in which the velocity at any given time fluctuates relative to space. It involves change in pressure, density and velocity over space and time (Bansal, 2004).

### 2.5.4 Compressible Flow and Incompressible Flow

A compressible flow occurs when the density of fluid fluctuates from a place to another or stated differently, is not constant. When the fluid's density remains constant and temperature and pressure variations hardly ever influence the fluid's volume, the flow is said to be incompressible. When examining how gases behave at high speeds, it is essential to understand compressible flow, whereas liquid and low speed gas flows are usually incompressible (Bansal, 2004).

### 2.5.5 Rotational and Irrotational Flow

When fluid particles rotate about their own axis while moving along stream lines, this is known as rotational flow. It entails the existence of whirling motion, circulatory flow patterns, or vortices. The flow is referred to as irrotational if the fluid particles show zero vorticity with no rotation about their axes while moving along stream lines (Bansal, 2004).

## 2.6 Newton's Law of Viscosity

Newton's law of viscosity emphasizes that the shear stress on elementary layer of fluid and shear strain is exactly proportional (Bansal, 2004).

## 2.7 Law of Mass Conservation

The law of mass conservation emphasizes that the total mass in a closed system always remains constant. Energy can only be moved from one system to another, it cannot be generated or dissipated (Crowell, 2001).

## 2.8 Law of Conservation of Energy

The law of conservation of energy emphasizes that the total energy in a closed system never changes over time. Energy can only be moved from one system to another, it cannot be generated or dissipated. The sum of the contributions from the system's properties, including motion of objects, heating of objects, and the relative positions of objects interacting through forces, yields the total energy (Crowell, 2001).

## 2.9 Dimensionless Numbers

### 2.9.1 Prandtl Number

In fluid mechanics, Prandtl number ($Pr$) is a parameter which is dimensionless, asserts that momentum diffusivity is divided by heat diffusivity (Kundu *et al.*, 2024).

$$Pr = \frac{Kinematic\ viscosity}{Heat\ diffusivity},$$

$$Pr = \frac{\nu}{\alpha}.$$

### 2.9.2 Reynolds Number

In fluid mechanics, Reynolds number is calculated by dividing inertial forces by viscous forces, that helps to estimate fluid's flow patterns in several scenarios. It is used to identify the laminar or turbulent flow type (Kundu *et al*., 2024).

$$Re = \frac{Inertial\ force}{Viscous\ force} = \frac{\rho sL}{\mu},$$

where $\mu$ is the dynamic viscosity, $\rho$ is density, $L$ is representing characteristic length and $s$ refers to flow speed.

### 2.9.3 Eckert Number

A nondimensional parameter, Eckert number ($Ec$) determines the proportion of kinetic energy to total heat alteration in the flow of fluid. The Eckert number is widely used in studies involving high-speed flows and serves the purpose to determine how kinetic energy impacts heat transfer.

$$Ec = \frac{c^2}{C_p \Delta T},$$

where $C_p$ is the constant velocity, $c$ refers to flow velocity and $\Delta T$ denotes the difference between local and wall temperature.

### 2.9.4 Darcy Number

The relative effect of medium's permeability over its cross sectional area is known as the Darcy number ($Da$) in fluid dynamics via porous media (Shruti et al., 2023).

$$Da = \frac{K}{d^2},$$

where $K$ denotes the medium's permeability and $d$ is the characteristic length here.

## 2.10 Basic Equations

### 2.10.1 Equation of Continuity

The continuity equation is the one that relies on the principle of conservation of mass. Therefore, the amount of fluid per second is constant for a fluid passing through the pipe at all cross sections (Bansal, 2004).

Mathematically,

$$\frac{\partial \rho}{\partial t} + \nabla.(\rho \boldsymbol{V}) = 0.$$

$\nabla.\boldsymbol{V} = \boldsymbol{0}$, when density remains constant.

### 2.10.2 Momentum Equation

The law of conservation of momentum, which asserts that the change in momentum of flow per unit of time in a given direction equals to the net force applied on a fluid mass, serves as the foundation of momentum equation (Bansal, 2004).

Mathematically, the momentum equation for incompressible fluid is expressed as

$$\rho \frac{d\boldsymbol{V}}{dt} = -\nabla \boldsymbol{p} + div\boldsymbol{S},$$

here, surface force is represented by $div\boldsymbol{S}$ and $\rho \frac{d\boldsymbol{V}}{dt}$ refers to local rate of change of momentum with time.

### 2.10.3 Energy Equation

The first law of thermodynamics, which is formulation of the law of conservation of energy, is the origin of the energy equation.

Mathematically, the energy equation for incompressible fluid is expressed as

$$\rho C_p \frac{dT}{dt} = -\nabla . \boldsymbol{q} + Tr(\boldsymbol{\tau} . \boldsymbol{L}),$$

where, total internal energy is represented by the term $\rho C_p \frac{dT}{dt}$, $\boldsymbol{\tau} . \boldsymbol{L}$ is viscous dissipation and $-\nabla . \boldsymbol{q}$ refers to heat flux.

## 2.11 Perturbation Method

Analytical methods used for finding approximate solutions of non-linear equations for which it is impossible to obtain exact solution are known as perturbation techniques. With this approach, difficult problem is broken down into a feasible one. It formulates the desired solution in terms of perturbation series by adding small parameter. Smallness and largeness of a given quantity can be determined by the perturbation parameters expressed as ε and δ. The solution to the exactly solvable problem is the leading term of perturbation series and remaining terms indicate the deviation in solution.

Perturbation techniques are frequently used across multiple fields including fluid dynamics, physics, quantum mechanics and celestial mechanics. The most challenging and developed applications of perturbation techniques found in quantum field theory. These techniques are also significant in illustrating, estimating and analyzing phenomena caused by non-linear operations in vibrating systems.

# CHAPTER 3

# ANALYZE A TEMPERATURE AND MHD PERISTALTIC FLOW OF SUTTERBY FLUID THROUGH A POROUS WAVE CHANNEL IN A ROTATING FRAME (Moeana & Al-Khafajy, 2024)

## 3.1 Introduction

This chapter offers a detailed review of work done by (Moeana & Al-Khafajy, 2024). They investigated the effects of rotation on the temperature and MHD peristaltically flowing non-Newtonian Sutterby fluid through porous wave medium. Assuming a low Reynolds number and long wavelength, perturbation technique was used to solve momentum equation. By using software "Mathematica 13", data was analyzed and graphs were obtained.

## 3.2 Mathematical Formulation

By considering Sutterby fluid peristaltically flowing through a porous wave channel, the equation for the flow channel wall in two-dimensional cartesian coordinates is given by

$$y^* = \pm\left[d^* - \varphi^* \sin\frac{2\pi}{\omega}(\bar{X} - st)\right], \tag{3.1}$$

where the channel's lower wall is represented by negative sign, and the upper wall by the positive sign. The average radius of the channel is denoted by $d^*$, the amplitude of a peristaltic wave by $\varphi^*$, the wavelength by $\omega$, the wave propagation speed by $s$, and the time by $t$.

An external magnetic field conducts electricity through the fluid given as $B = (0, B_0, 0)$. Around the z-axis, the fluid rotates at a constant angular velocity $\Omega$. The fluid flows peristaltically in the middle of the channel because of the wave motion of the flow channel wall (contraction and relaxation). $(\bar{V}_1, \bar{V}_3)$ are velocity components and $\bar{p}$ represents pressure.

The extra stress tensor $\tau$ of Sutterby fluid is

$$\tau = \frac{\mu}{2}\left[\frac{\sinh^{-1} b\hat{\gamma}}{b\hat{\gamma}}\right]^{n}(\nabla\overline{V} + (\nabla\overline{V})^{T}), \tag{3.2}$$

where velocity field is denoted by $\bar{V}$, $\nabla\bar{V}$ is fluid velocity's gradient, $\mu$ refers to zero-shear rate viscosity and second invariant strain tensor is denoted by $\hat{\gamma}$ which is defined as

$$\hat{\gamma} = \sqrt{\frac{1}{2}\, tr(\nabla\overline{V} + (\nabla\overline{V})^{T})^{2}}. \tag{3.3}$$

When $|b\hat{\gamma}| \ll 1$, then $\sinh^{-1}(b\hat{\gamma}) \approx (b\hat{\gamma}) - \frac{(b\hat{\gamma})^{3}}{6}$

Equation (3.2) becomes

$$\tau \approx \frac{\mu}{2}\left[1 - \frac{nb^{2}}{6}(\hat{\gamma})^{2}\right](\nabla\overline{V} + (\nabla\overline{V})^{T}). \tag{3.4}$$

Now we know that,,

$$(\nabla\overline{V} + (\nabla\overline{V})^{T}) = \begin{bmatrix} 2\frac{\partial\overline{V}_1}{\partial\bar{X}} & \frac{\partial\overline{V}_1}{\partial\bar{Y}} + \frac{\partial\overline{V}_3}{\partial\bar{X}} \\ \frac{\partial\overline{V}_1}{\partial\bar{Y}} + \frac{\partial\overline{V}_3}{\partial\bar{X}} & 2\frac{\partial\overline{V}_3}{\partial\bar{Y}} \end{bmatrix}, \tag{3.5}$$

$$\hat{\gamma} = \sqrt{2\left(\frac{\partial\overline{V}_1}{\partial\bar{X}}\right)^{2} + \left(\frac{\partial\overline{V}_1}{\partial\bar{Y}} + \frac{\partial\overline{V}_3}{\partial\bar{X}}\right)^{2} + 2\left(\frac{\partial\overline{V}_3}{\partial\bar{Y}}\right)^{2}}\,. \tag{3.6}$$

The component of tensor is,

$$\bar{\tau}_{\bar{X}\bar{Y}} = \frac{\mu}{2}\left[1 - \frac{nb^{2}}{6}\left(2\left(\frac{\partial\overline{V}_1}{\partial\bar{X}}\right)^{2} + \left(\frac{\partial\overline{V}_1}{\partial\bar{Y}} + \frac{\partial\overline{V}_3}{\partial\bar{X}}\right)^{2} + 2\left(\frac{\partial\overline{V}_3}{\partial\bar{Y}}\right)^{2}\right)\right]\left(\frac{\partial\overline{V}_1}{\partial\bar{Y}} + \frac{\partial\overline{V}_3}{\partial\bar{X}}\right). \tag{3.7}$$

The governing equations for the Sutterby fluid model's flow problem are given as

Equation of Continuity

$$\frac{\partial\overline{V}_1}{\partial\bar{X}} + \frac{\partial\overline{V}_3}{\partial\bar{Y}} = 0. \tag{3.8}$$

The x- component of Momentum equation is

$$\rho\left(\frac{\partial \bar{V}_1}{\partial \bar{t}} + \bar{V}_1 \frac{\partial \bar{V}_1}{\partial \bar{X}} + \bar{V}_3 \frac{\partial \bar{V}_1}{\partial \bar{Y}}\right) - \Omega\rho\bar{V}_1 = -\frac{\partial \bar{P}}{\partial \bar{X}} + \frac{\partial \bar{\tau}_{\bar{X}\bar{X}}}{\partial \bar{X}} + \frac{\partial \bar{\tau}_{\bar{X}\bar{Y}}}{\partial \bar{Y}} - \sigma {B_0}^2 \bar{V}_1 - \frac{\mu}{\hat{K}}\bar{V}_1. \quad (3.9)$$

The y- component of Momentum equation is

$$\rho\left(\frac{\partial \bar{V}_3}{\partial \bar{t}} + \bar{V}_1 \frac{\partial \bar{V}_3}{\partial \bar{X}} + \bar{V}_3 \frac{\partial \bar{V}_3}{\partial \bar{Y}}\right) - \Omega\rho\bar{V}_3 = -\frac{\partial \bar{P}}{\partial \bar{Y}} + \frac{\partial \bar{\tau}_{\bar{Y}\bar{X}}}{\partial \bar{X}} + \frac{\partial \bar{\tau}_{\bar{Y}\bar{Y}}}{\partial \bar{Y}} - \frac{\mu}{\hat{K}}\bar{V}_3. \quad (3.10)$$

The Energy equation is

$$\rho C_p\left(\frac{\partial T}{\partial \bar{t}} + \bar{V}_1 \frac{\partial T}{\partial \bar{X}} + \bar{V}_3 \frac{\partial T}{\partial \bar{Y}}\right) = H\left(\frac{\partial^2 T}{\partial \bar{X}^2} + \frac{\partial^2 T}{\partial \bar{Y}^2}\right) + \frac{\partial \bar{V}_1}{\partial \bar{X}}\bar{\tau}_{\bar{X}\bar{X}} + \frac{\partial \bar{V}_1}{\partial \bar{Y}}\bar{\tau}_{\bar{X}\bar{Y}} + \frac{\partial \bar{V}_3}{\partial \bar{X}}\bar{\tau}_{\bar{Y}\bar{X}} + \frac{\partial \bar{V}_3}{\partial \bar{Y}}\bar{\tau}_{\bar{Y}\bar{Y}} - G(T - T_0). \quad (3.11)$$

where $\Omega$ is rotation parameter, $B_0$ represents applied magnetic field, $\sigma$ represents electric conductivity, $\hat{K}$ refer to permeability, $\rho$ is fluid density, specific heat is represented by $C_p$, $H$ refer to thermal conductivity and heat source is represented by $G$.

The relations to convert $(\bar{X}, \bar{Y})$ to the $(\bar{x}, \bar{y})$ are given by,

$$\bar{v}_1(\bar{x}, \bar{y}) = \bar{V}_1(\bar{X} - s\bar{t}, \bar{Y}, \bar{t}) - s, \quad \bar{v}_3(\bar{x}, \bar{y}) = \bar{V}_3(\bar{X} - s\bar{t}, \bar{Y}, \bar{t}), \quad \bar{p}(\bar{x}, \bar{y}) = \bar{P}(\bar{X} - s\bar{t}, \bar{Y}, \bar{t}). \quad (3.12)$$

The dimensionless quantities utilized are:

$$x = \frac{\bar{x}}{\omega}, \; y = \frac{\bar{y}}{d_1}, \; v_1 = \frac{\bar{v}_1}{s}, \; v_3 = \frac{\omega \bar{v}_3}{s d_1}, p = \frac{{d_1}^2 \bar{p}}{\mu \omega s}, Re = \frac{\rho s d_1}{\mu}, \varepsilon = \frac{n b^2 s^2}{2{d_1}^2},$$

$$\delta = \frac{d_1}{\omega}, \varphi = \frac{\bar{\varphi}}{d_1}, \; \tau_{xx} = \frac{\bar{\tau}_{\bar{x}\bar{x}}}{\mu s}, \; \tau_{xy} = \frac{\bar{\tau}_{\bar{x}\bar{y}}}{\mu s}, \; \tau_{yy} = \frac{\bar{\tau}_{\bar{y}\bar{y}}}{\mu s}, \; \theta = \frac{T - T_0}{T_1 - T_0},$$

$$Me^2 = \frac{{d_1}^2}{\mu}\sigma {B_0}^2, \; Hc = \frac{G{d_1}^2}{\mu C_p}, \; Da = \frac{\hat{K}}{{d_1}^2}, \; Pr = \frac{\mu c_p}{H}, Ec = \frac{s^2}{C_p(T - T_0)}, \quad (3.13)$$

where $Pr$ is Prandtl number, $Ec$ is Eckert number, $Da$ is Darcy number, $Re$ is Reynolds number, $Hc$ is heat source parameter, $\epsilon$ is sutterby fluid parameter, $\delta$ is dimensionless wave number and $Me$ is magnetic parameter. Dimensionless temperature and amplitude ratio are given by $\theta$ and φ respectively.

After the non-dimensional analysis, the system obtained is

$$\frac{\partial v_1}{\partial x} + \frac{\partial v_3}{\partial y} = 0, \tag{3.14}$$

$$Re\delta\left(v_1 \frac{\partial v_1}{\partial x} + v_3 \frac{\partial v_1}{\partial y}\right) - \frac{\rho {d_1}^2}{\mu}\Omega(v_1 + 1) = -\frac{\partial p}{\partial x} + \delta^2 \frac{\partial \tau_{xx}}{\partial x} + \frac{\partial \tau_{xy}}{\partial y} - \left(Me^2 + \frac{1}{Da}\right)(v_1 + 1),$$

(3.15)

$$Re\delta^3\left(v_1 \frac{\partial v_3}{\partial x} + v_3 \frac{\partial v_3}{\partial y}\right) - \delta^2 \frac{\rho {d_1}^2}{\mu}\Omega v_3 = -\frac{\partial p}{\partial y} + \delta^2 \frac{\partial \tau_{yx}}{\partial x} + \delta^2 \frac{\partial \tau_{yy}}{\partial y} - \delta^2 \frac{1}{Da} v_3, \tag{3.16}$$

$$Re\delta\left(v_1 \frac{\partial \theta}{\partial x} + v_3 \frac{\partial \theta}{\partial y}\right) = \frac{1}{Pr}\left(\delta^2 \frac{\partial^2 \theta}{\partial x^2} + \frac{\partial^2 \theta}{\partial y^2}\right) + Ec\left(\delta^2 \frac{\partial v_1}{\partial x}(\tau_{xx}) + \frac{\partial v_1}{\partial y}(\tau_{xy}) + \delta^2 \frac{\partial v_3}{\partial x}(\tau_{yx}) + \delta^2 \frac{\partial v_3}{\partial y}(\tau_{yy})\right) - Hc\theta. \tag{3.17}$$

Component of extra stress tensor is

$$\tau_{xy} = \left[1 - \epsilon\left\{2\delta^2\left(\frac{\partial v_1}{\partial x}\right)^2 + \left(\frac{\partial v_1}{\partial y} + \delta^2 \frac{\partial v_3}{\partial x}\right)^2 + 2\delta^2\left(\frac{\partial v_3}{\partial y}\right)^2\right\}\right]\left(\frac{\partial v_1}{\partial y} + \delta^2 \frac{\partial v_3}{\partial x}\right). \tag{3.18}$$

The associated dimensionless boundary conditions are

$$v_1 = -1 \quad at \quad y^* = \pm w = \pm(1 - \varphi^* \sin 2\pi x),$$

$$\theta = 0 \quad at \quad y^* = -w = -1 + \varphi^* \sin 2\pi x,$$

$$\theta = 1 \quad at \quad y^* = w = 1 - \varphi^* \sin 2\pi x.$$

By assuming wavelength to be small ($\delta \ll 1$) and applying lubrication approach we get

$$-\frac{\rho {d_1}^2}{\mu}\Omega(v_1 + 1) = -\frac{\partial p}{\partial x} + \frac{\partial \tau_{xy}}{\partial y} - \left(Me^2 + \frac{1}{Da}\right)(v_1 + 1), \tag{3.19}$$

$$\frac{\partial p}{\partial y} = 0, \tag{3.20}$$

$$\frac{1}{Pr}\frac{\partial^2 \theta}{\partial y^2} + Ec\ \tau_{xy}\left(\frac{\partial v_1}{\partial y}\right) - Hc\theta = 0, \tag{3.21}$$

$$\tau_{xy} = \left[\frac{\partial v_1}{\partial y} - \varepsilon\left(\frac{\partial v_1}{\partial y}\right)^3\right]. \tag{3.22}$$

By substituting equation (3.22) in (3.19), we obtain:

$$-\frac{\rho {d_1}^2}{\mu}\Omega(v_1 + 1) = -\frac{\partial p}{\partial x} + \frac{\partial^2 v_1}{\partial y^2} - 3\varepsilon\left(\frac{\partial v_1}{\partial y}\right)^2 \frac{\partial^2 v_1}{\partial y^2} - \left(Me^2 + \frac{1}{Da}\right)(v_1 + 1), \tag{3.23}$$

In fixed coordinate system, the real time flow rate is determined by

$$\hat{Q} = \int_{-w}^{w} \bar{V}_1(\bar{X} - s\bar{t}, \bar{Y}, \bar{t})d\bar{Y}. \tag{3.24}$$

Using transformation in equation (3.13) and intergrating it, we obtain

$$\hat{Q} = \bar{q} + 2sw. \tag{3.25}$$

Where $\bar{q} = \int_{-w}^{w} \bar{v}_1(\bar{x}, \bar{y})d\bar{y}$.

The flow rate over a period $T = \frac{\omega}{s}$ at a fixed position is defined as

$$\bar{Q} = \frac{1}{T}\int_0^T \hat{Q}d\bar{t}. \tag{3.26}$$

By substituting equation (3.25) in equation (3.26), we get

$$\bar{Q} = \frac{1}{T}\int_0^T (\bar{q} + 2sw)d\bar{t} = \bar{q} + 2s\left(d - \frac{\bar{\emptyset}}{2}\right). \tag{3.27}$$

By using equation (3.13) into equation (3.27)

$$dsQ = dsq + 2s\left(d - \frac{d\bar{\emptyset}}{2}\right). \tag{3.28}$$

The non dimensional equation (3.28) is

$$Q = q + 2 - \emptyset,$$

$$\text{then } q = Q + \emptyset - 2,$$

where q refers to non dimensional volume flow rate in the wave frame and takes the following form

$$dsq = \int_{-w}^{w} sv_1 \, d \, dy,$$

$$q = \int_{-w}^{w} v_1 \, dy.$$

## 3.3 Solution Methodology

By solving, equation (3.23) becomes

$$\frac{\partial^2 v_1}{\partial y^2} - Av_1 = \frac{\partial p}{\partial x} + 3\varepsilon \left(\frac{\partial v_1}{\partial y}\right)^2 \frac{\partial^2 v_1}{\partial y^2} + A, \tag{3.29}$$

with

$$A = Me^2 + \frac{1}{Da} - \frac{\rho {d_1}^2}{\mu} \Omega.$$

To find the problem solution, Perturbation technique is used. Using the small parameter

$\varepsilon \ll 1$, we open the perturbation series as

$$v_1 = v_{10} + \varepsilon v_{11} + O(\varepsilon^2),$$

$$p = p_0 + \varepsilon p_1 + O(\varepsilon^2). \tag{3.30}$$

### 3.3.1 Zeroth Order System $(\boldsymbol{\varepsilon^0})$

$$\frac{\partial^2 v_{10}}{\partial y^2} - Av_{10} = \frac{dp_0}{dx} + A, \tag{3.31}$$

with corresponding boundary conditions

$$v_{10} = -1, \quad at \quad y^* = \pm w = \pm(1 - \varphi^* \sin 2\pi x)$$

### 3.3.2 First Order System $(\boldsymbol{\varepsilon^1})$

$$\frac{\partial^2 v_{11}}{\partial y^2} - A v_{11} = \frac{dp_1}{dx} + 3\left(\frac{\partial v_{10}}{\partial y}\right)^2 \frac{\partial^2 v_{10}}{\partial y^2}, \tag{3.32}$$

with corresponding boundary conditions:

$$v_{11} = 0, \quad at \quad y^* = \pm w = \pm(1 - \varphi^* \sin 2\pi x).$$

## 3.4 Result and Discussions

Figures $3.1 - 3.6$ showing the effects of rotation parameter $\Omega$, porosity parameter $Da$, magnetic parameter $Me$, Sutterby fluid parameter $\epsilon$, $\phi$ and $Q_0, Q_1$. The conduct of different factors on pressure gradient are plotted in figures $3.7 - 3.10$. Plots illustrating the impacts of different parameters on the temperature distribution can be seen in figures $3.11 - 3.14$.

Figure 3.1 shows that the velocity $v_1$ rises as the rotation parameter $\Omega$ increases. Increase in rotation parameter enhances the centrifugal force which tends the fluid in the center of the channel to surge in velocity. Figure 3.2 shows how the velocity $v_1$ changes as the porosity parameter value changes. The fluid velocity near the channel center increases as $Da$ rises because the flow resistance falls but near the walls, fluid velocity decreases. The variation of magnetic parameter $Me$ on the velocity component $v_1$ is shown in Figure 3.3. The fluid flow is opposed by a resistive force generated by the applied magnetic field. This resistive effect grows with the magnetic parameter, reducing the velocity's magnitude at the channel's center.

Figure 3.4 illustrates how the velocity profile is affected by Sutterby fluid parameter $\epsilon$. Improved shear thinning effects which are correlated with a surge in $\epsilon$, reduce the resistance of fluid to flow under deformation and results in higher velocity at channel's center. For different values of parameter $\phi$, figure 3.5 plots the fluctuation of velocity component $v_1$ along the y-axis. Rise in $\phi$ improves momentum diffusion and heat conductivity, which lowers flow resistance due to which velocity increases. The rise in velocity is relatively small because heat enhancement and viscosity have opposing effects.

Figure 3.6 is showing the variation of different values of the parameter $Q_0, Q_1$ on the velocity component $v_1$ along the y-axis. Velocity profile is enhanced, practically near to centerline by an increase in $Q_0, Q_1$, which indicates increased internal heat generation. As a result, a rise in $Q_0, Q_1$ leads to higher velocity at the channel's center.

The fluctuation of the pressure gradient $\frac{dp}{dx}$ for various values of Darcy number ($Da$) can be seen in Figure 3.7. $Da$ represents the porous medium's Permeability. Resistance to the flow of fluid decreases with higher $Da$ due to more open pore space, which lowers the value of pressure gradient. Figure 3.8 shows how pressure gradient $\frac{dp}{dx}$ changes for different values of magnetic parameter. As $Me$ rises, magnetic field employs a Lorentz force that opposes the fluid flow which results in higher pressure gradient values. The pressure gradient's fluctuation for various rotation parameter values is shown in figure 3.9. Reduced values of the pressure gradient are the result of stronger Coriolis effects caused by a surge in rotation parameter, which also lessens flow resistance. Figure 3.10 illustrates how increasing the Sutterby fluid parameter $\epsilon$ drives the pressure gradient to decrease. It indicates that a greater value of $\epsilon$ reduces flow resistance, which lowers the pressure gradient for all values.

The temperature profile can be seen in figure 3.11 for a range of Sutterby fluid parameter $\epsilon$ values. Fluid shows better shear thinning behavior as $\epsilon$ rises, leads to decreased thermal boundary layer thickness and more effective heat transmission. In turn, the fluid's temperature drops. The temperature variation for various rotation parameter values is depicted in the figure 3.12. As the rotation parameter $\Omega$ rises, the fluid experiences rotational motion and stronger fluid mixing. Which enhances heat dissipation and as a result, the temperature slightly falls. Consequently, temperature profile lowers. Figure 3.13 illustrate how the temperature changes for various magnetic parameter ($Me$) values. A Lorentz force is produced when magnetic field is applied, which opposes fluid flow and slows fluid motion. As there is lower convective heat transfer due to reduced velocity, the temperature distribution is higher. The temperature variations for different porosity parameter ($Da$) values can be seen in figure 3.14. The resistance to flow lowers as porosity parameter $Da$ rises, improving thermal energy storage and causing the fluid to cool more slowly, ultimately leading to higher fluid temperature.

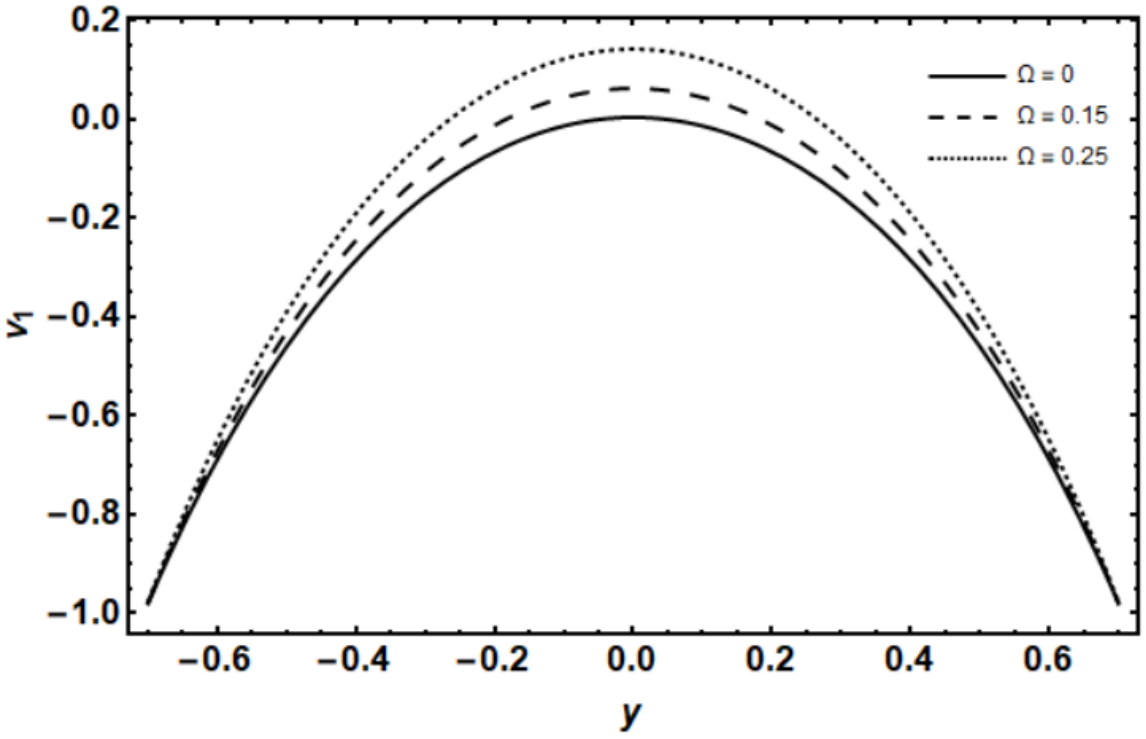


**Figure 3.1** Velocity variation for the rotation parameter.

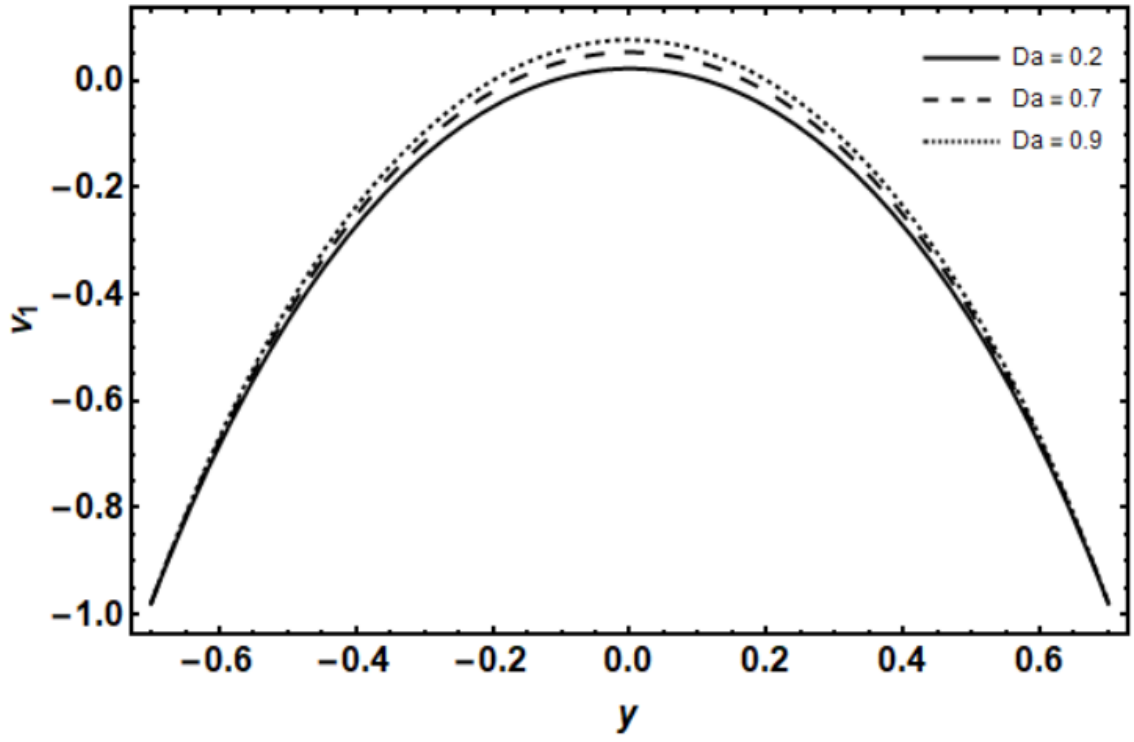


**Figure 3.2** Velocity variation for the porosity parameter.

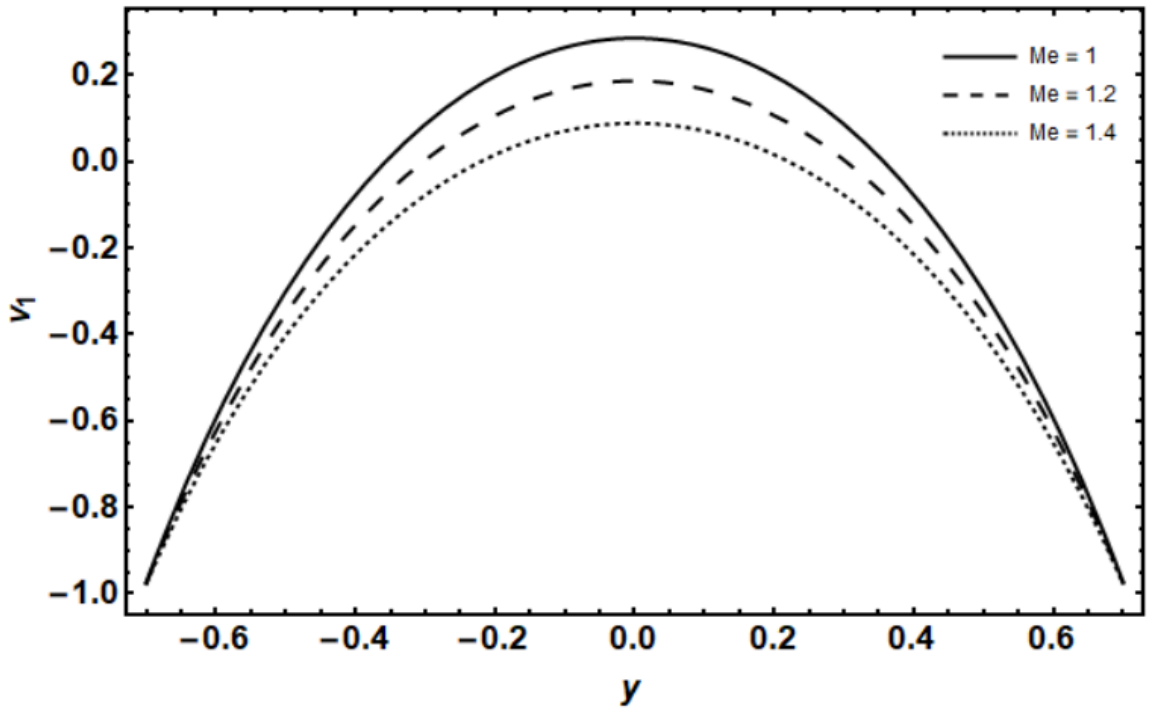


**Figure 3.3** Velocity variation for the magnetic parameter.

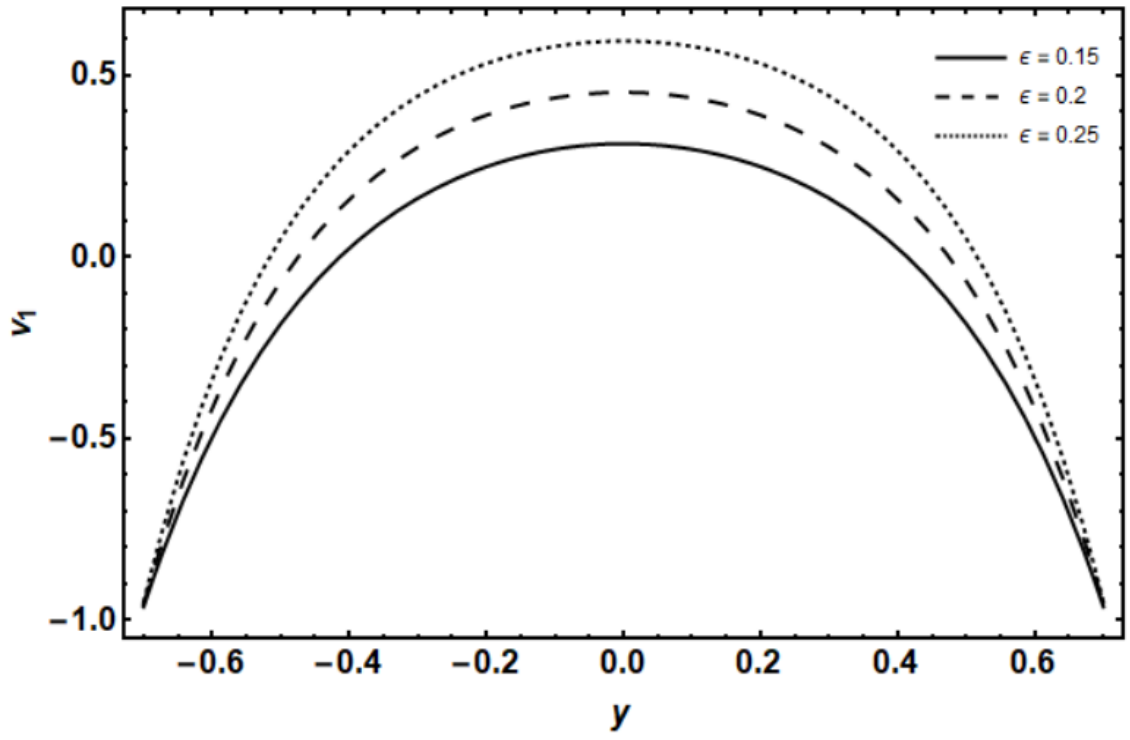


**Figure 3.4** Variation of Sutterby fluid parameter $\epsilon$ on the velocity.

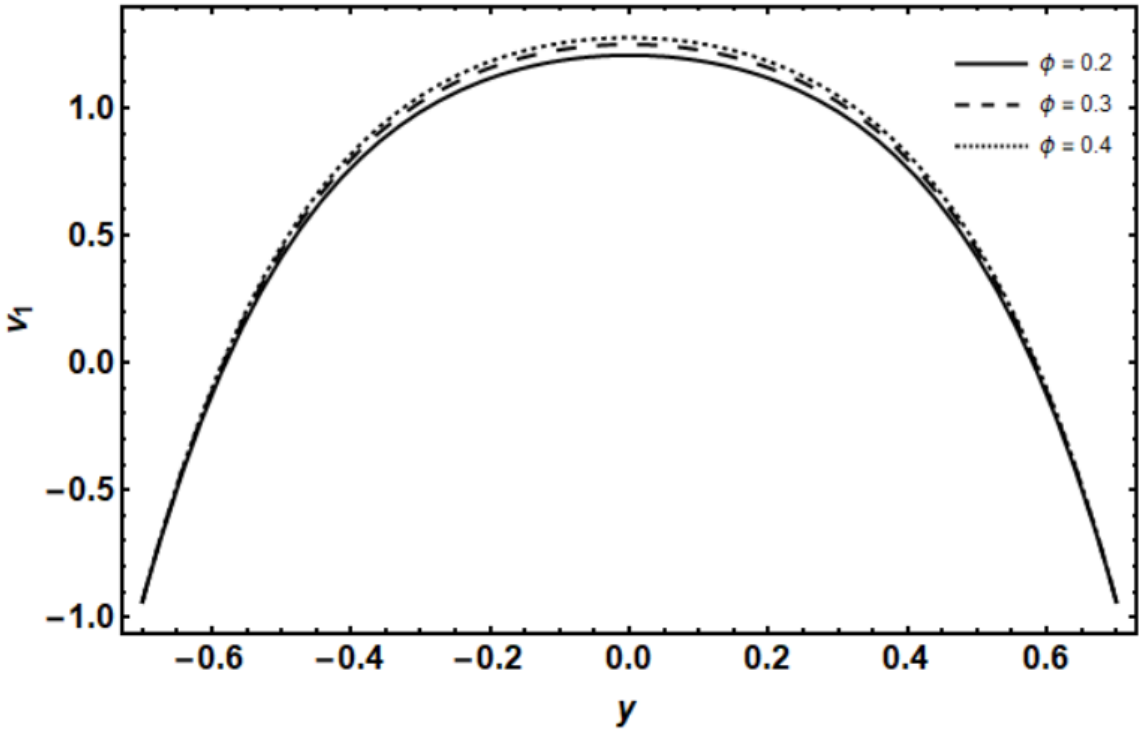


**Figure 3.5** Variation of $\phi$ on the velocity.

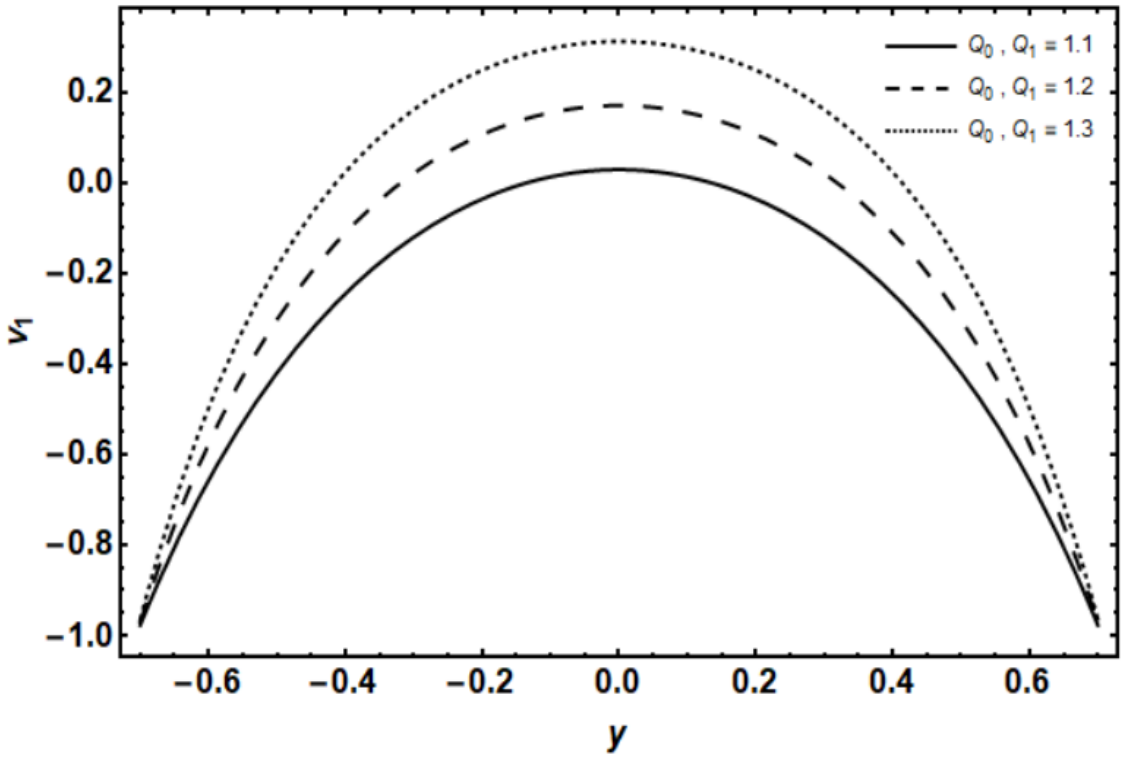


**Figure 3.6** $Q_0, Q_1$ variations on the velocity.

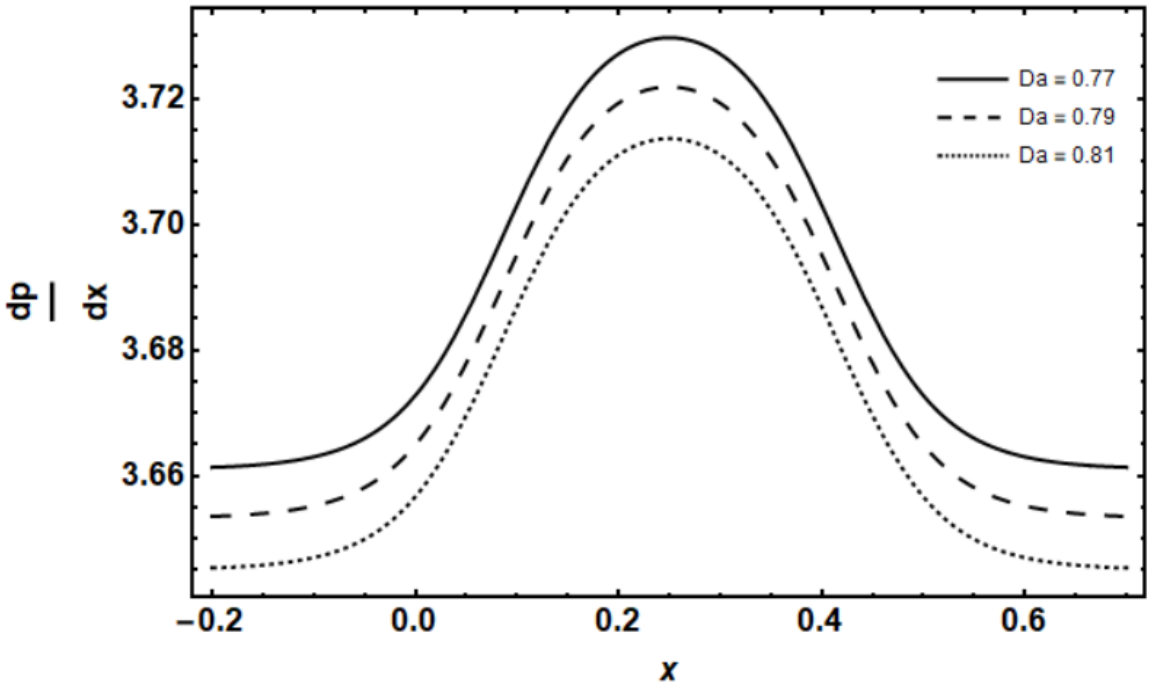


**Figure 3.7** Variation of porosity parameter on pressure gradient.

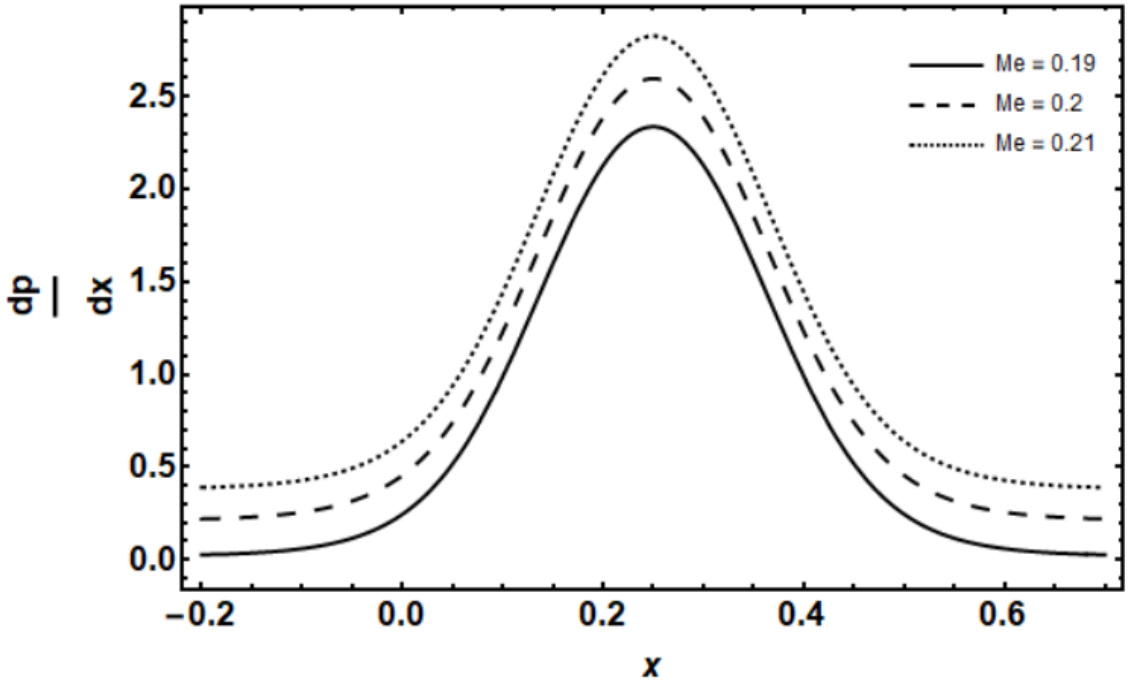


**Figure 3.8** Variation of Magnetic parameter on pressure gradient.

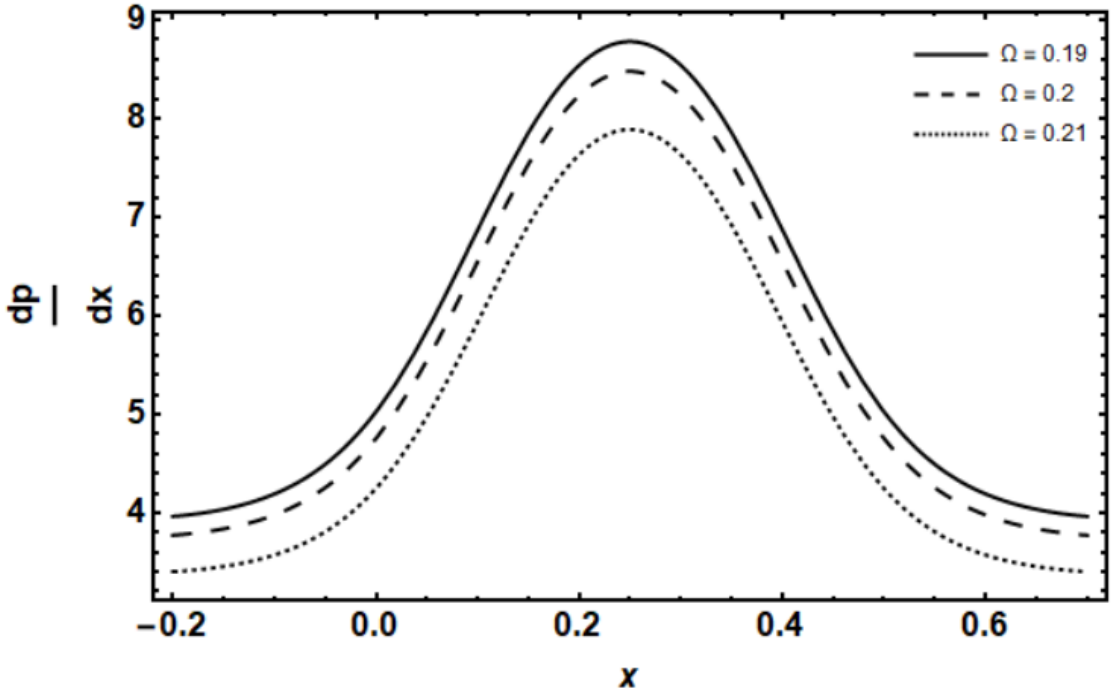


**Figure 3.9** Variation of rotation parameter on pressure gradient.

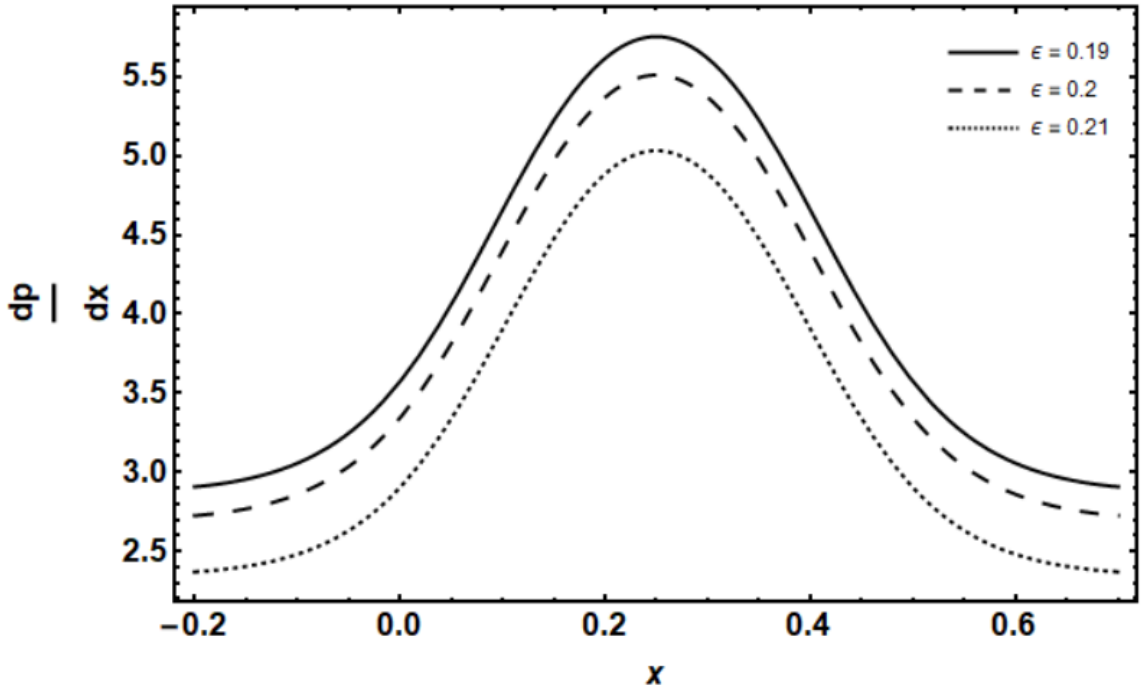


**Figure 3.10** Variation of $\epsilon$ on pressure gradient.

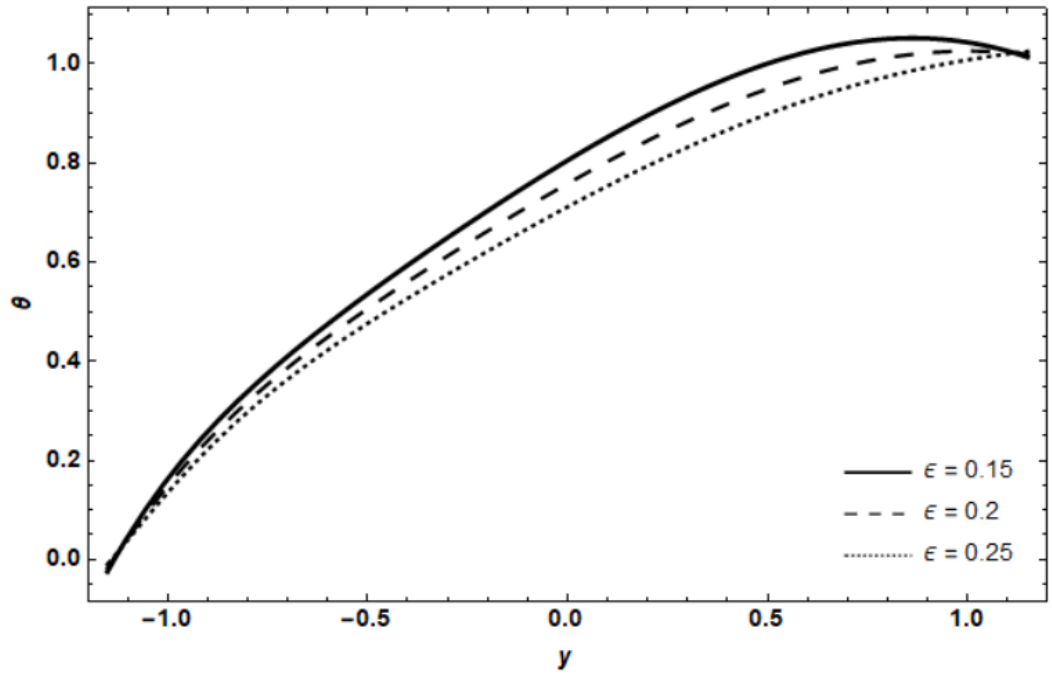


**Figure 3.11** Temperature variation for the Sutterby fluid parameter $\epsilon$.

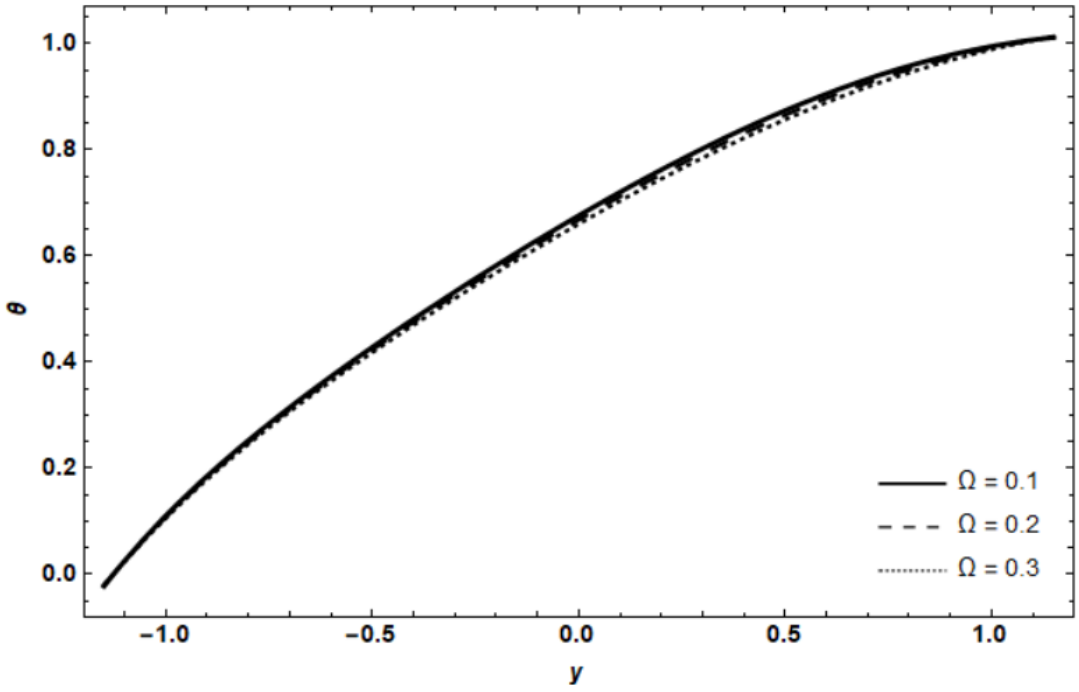


**Figure 3.12** Temperature variation for the $\Omega$.

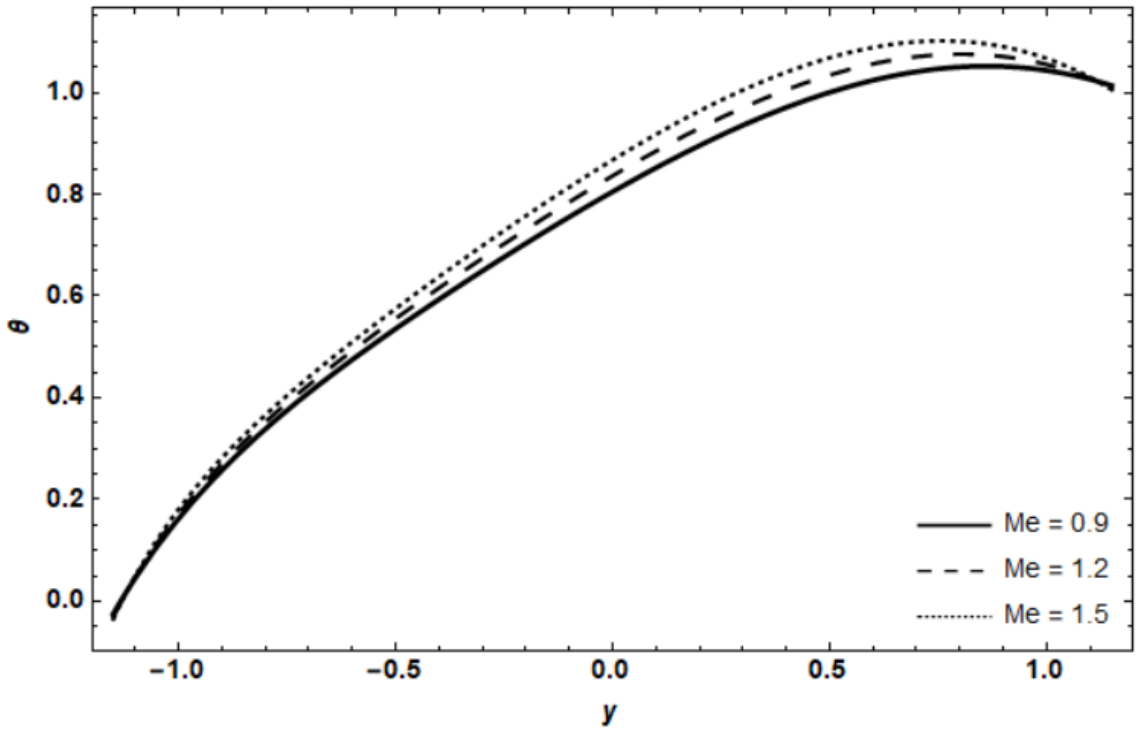


**Figure 3.13** Temperature variation for the $Me$.

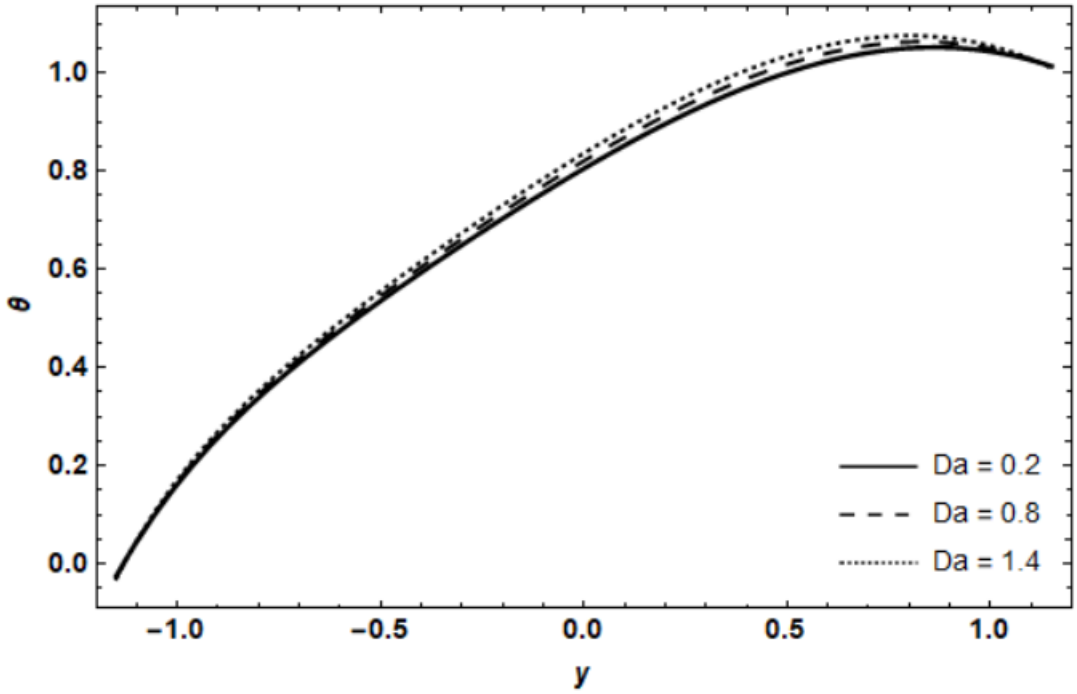


**Figure 3.14** Temperature variation for the $Da$.

# CHAPTER 4

# EFFECTS OF POROUS ROTATING FRAME ON PERISTALTIC MHD JEFFREY FLUID FLOW

## 4.1 Introduction

Chapter 4 extends the review work by (Moeana & Al-Khafajy, 2024). In this system, we are considering Jeffrey fluid model instead of Sutterby fluid model. This study investigates the impact of rotation on a non-Newtonian Jeffrey fluid's temperature and magnetohydrodynamic peristaltic flow in a porous medium. The system of equations is non-homogeneous and non-linear partial differential stated in the cartesian coordinates. The momentum problem is solved using the perturbation method, assuming a very low Reynolds number and long wavelength. The program "Mathematica 13" is used to analyse data and generate graphs.

## 4.2 Mathematical Formulation

Considering Jeffrey fluid flow peristaltically in two dimensional cartesian coordinates through porous wave channel.

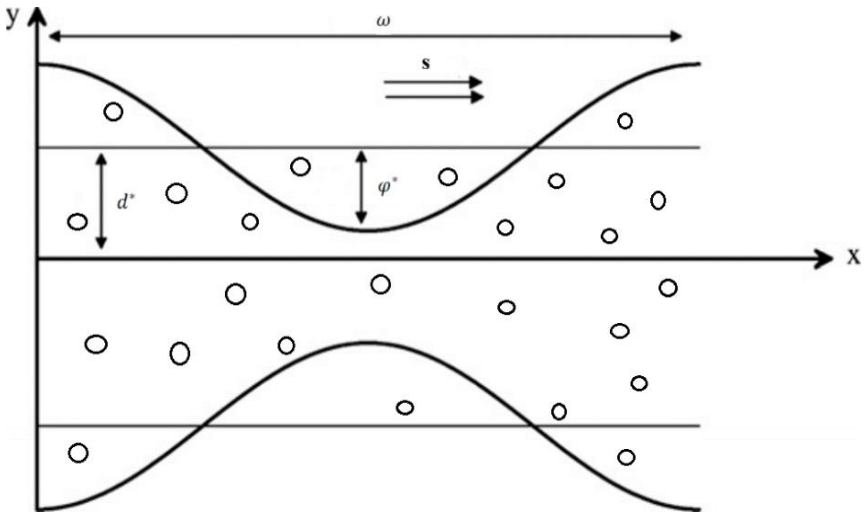


**Figure a**: The geometry of the problem.

The equation for flow channel wall is given by

$$y^* = \pm\left[d^* - \varphi^* \sin\frac{2\pi}{\omega}(\bar{X} - st)\right], \tag{4.1}$$

where the upper wall is denoted by positive sign and lower wall of channel is denoted by negative sign. $d^*$ refers to average radius of channel, the peristaltic wave's amplitude is represented by $\varphi^*$, wavelength is indicated by $\omega$, $s$ represents the wave propagation speed and $t$ refers to time. $(\bar{V}_1, \bar{V}_3)$ are velocity components and $\bar{p}$ represents pressure.

The components of tensor of Jeffrey fluid model are given by

$$\bar{\tau}_{\bar{X}\bar{X}} = \frac{2\mu}{1+\lambda_1}\left(1 + \lambda_2\left(\frac{\partial}{\partial t} + \bar{V}_1\frac{\partial}{\partial \bar{X}} + \bar{V}_3\frac{\partial}{\partial \bar{Y}}\right)\right)\frac{\partial \bar{V}_1}{\partial \bar{X}}, \tag{4.2}$$

$$\bar{\tau}_{\bar{X}\bar{Y}} = \frac{\mu}{1+\lambda_1}\left(1 + \lambda_2\left(\frac{\partial}{\partial t} + \bar{V}_1\frac{\partial}{\partial \bar{X}} + \bar{V}_3\frac{\partial}{\partial \bar{Y}}\right)\right)\left(\frac{\partial \bar{V}_1}{\partial \bar{Y}} + \frac{\partial \bar{V}_3}{\partial \bar{X}}\right), \tag{4.3}$$

$$\bar{\tau}_{\bar{Y}\bar{Y}} = \frac{2\mu}{1+\lambda_1}\left(1 + \lambda_2\left(\frac{\partial}{\partial t} + \bar{V}_1\frac{\partial}{\partial \bar{X}} + \bar{V}_3\frac{\partial}{\partial \bar{Y}}\right)\right)\frac{\partial \bar{V}_3}{\partial \bar{Y}}. \tag{4.4}$$

The governing equations in two dimensions for the Jeffrey fluid model's flow problem is given as:

The Continuity equation is

$$\frac{\partial \bar{V}_1}{\partial \bar{X}} + \frac{\partial \bar{V}_3}{\partial \bar{Y}} = 0. \tag{4.5}$$

The x- component of Momentum equation is

$$\rho\left(\frac{\partial \bar{V}_1}{\partial \bar{t}} + \bar{V}_1\frac{\partial \bar{V}_1}{\partial \bar{X}} + \bar{V}_3\frac{\partial \bar{V}_1}{\partial \bar{Y}}\right) - \Omega\rho\bar{V}_1 = -\frac{\partial \bar{P}}{\partial \bar{X}} + \frac{\partial \bar{\tau}_{\bar{X}\bar{X}}}{\partial \bar{X}} + \frac{\partial \bar{\tau}_{\bar{X}\bar{Y}}}{\partial \bar{Y}} - \sigma {B_0}^2\bar{V}_1 - \frac{\mu}{\bar{K}}\bar{V}_1. \tag{4.6}$$

The y- component of Momentum equation is

$$\rho\left(\frac{\partial \bar{V}_3}{\partial \bar{t}} + \bar{V}_1\frac{\partial \bar{V}_3}{\partial \bar{X}} + \bar{V}_3\frac{\partial \bar{V}_3}{\partial \bar{Y}}\right) - \Omega\rho\bar{V}_3 = -\frac{\partial \bar{P}}{\partial \bar{Y}} + \frac{\partial \bar{\tau}_{\bar{Y}\bar{X}}}{\partial \bar{X}} + \frac{\partial \bar{\tau}_{\bar{Y}\bar{Y}}}{\partial \bar{Y}} - \frac{\mu}{\bar{K}}\bar{V}_3. \tag{4.7}$$

The Energy equation is

$$\rho C_p\left(\frac{\partial T}{\partial \bar{t}}+\bar{V}_1\frac{\partial T}{\partial \bar{X}}+\bar{V}_3\frac{\partial T}{\partial \bar{Y}}\right)=H\left(\frac{\partial^2 T}{\partial \bar{X}^2}+\frac{\partial^2 T}{\partial \bar{Y}^2}\right)+\frac{\partial \bar{V}_1}{\partial \bar{X}}\bar{\tau}_{\bar{X}\bar{X}}+\frac{\partial \bar{V}_1}{\partial \bar{Y}}\bar{\tau}_{\bar{X}\bar{Y}}+\frac{\partial \bar{V}_3}{\partial \bar{X}}\bar{\tau}_{\bar{Y}\bar{X}}+\frac{\partial \bar{V}_3}{\partial \bar{Y}}\bar{\tau}_{\bar{Y}\bar{Y}}-G(T-T_0). \tag{4.8}$$

where $\Omega$ represents rotation parameter, $B_0$ is applied magnetic field, $\sigma$ denotes electric conductivity, $\widehat{K}$ is permeability, $\rho$ refers to fluid density, specific heat is represented by $C_p$, $H$ refer to thermal conductivity and heat source is represented by $G$.

The relations to convert $(\bar{X},\bar{Y})$ to the $(\bar{x},\bar{y})$ are given by

$$\bar{v}_1(\bar{x},\bar{y})=\bar{V}_1(\bar{X}-s\bar{t},\bar{Y},\bar{t})-s,\quad \bar{v}_3(\bar{x},\bar{y})=\bar{V}_3(\bar{X}-s\bar{t},\bar{Y},\bar{t}),\quad \bar{p}(\bar{x},\bar{y})=\bar{P}(\bar{X}-s\bar{t},\bar{Y},\bar{t}). \tag{4.9}$$

The dimensionless quantities are given as

$$x=\frac{\bar{x}}{\omega},\ y=\frac{\bar{y}}{d_1},\ v_1=\frac{\bar{v}_1}{s},\ v_3=\frac{\omega\bar{v}_3}{sd_1},p=\frac{{d_1}^2\bar{p}}{\mu\omega s},Re=\frac{\rho s d_1}{\mu},\varepsilon=\frac{nb^2s^2}{2{d_1}^2},$$

$$\delta=\frac{d_1}{\omega},\varphi=\frac{\bar{\varphi}}{d_1},\ \tau_{xx}=\frac{\bar{\tau}_{\bar{x}\bar{x}}}{\mu s},\ \tau_{xy}=\frac{\bar{\tau}_{\bar{x}\bar{y}}}{\mu s},\ \tau_{yy}=\frac{\bar{\tau}_{\bar{y}\bar{y}}}{\mu s},\ \theta=\frac{T-T_0}{T_1-T_0},\ Me^2=\frac{{d_1}^2}{\mu}\sigma{B_0}^2,$$

$$Hc=\frac{G{d_1}^2}{\mu c_p},Da=\frac{\widehat{K}}{{d_1}^2},Pr=\frac{\mu c_p}{H},Ec=\frac{s^2}{c_p(T-T_0)},\quad \eta=1+\varphi^*\sin 2\pi x. \tag{4.10}$$

$Pr$ is Prandtl number, $Da$ is Darcy number, $Re$ is Reynolds number, $Hc$ is heat source parameter, $Ec$ is Eckert number, $\delta$ is dimensionless wave number and $Me$ is magnetic parameter. Dimensionless temperature and amplitude ratio are given by $\theta$ and φ respectively.

The non-dimensional system of governing equations is

$$\frac{\partial v_1}{\partial x}+\frac{\partial v_3}{\partial y}=0, \tag{4.11}$$

$$Re\delta\left(v_1\frac{\partial v_1}{\partial x}+v_3\frac{\partial v_1}{\partial y}\right)-\frac{\rho{d_1}^2}{\mu}\Omega(v_1+1)=-\frac{\partial p}{\partial x}+\delta^2\frac{\partial \tau_{xx}}{\partial x}+\frac{\partial \tau_{xy}}{\partial y}-\left(Me^2+\frac{1}{Da}\right)(v_1+1),$$

(4.12)

$$Re\delta^3\left(v_1\frac{\partial v_3}{\partial x}+v_3\frac{\partial v_3}{\partial y}\right)-\delta^2\frac{\rho {d_1}^2}{\mu}\Omega v_3=-\frac{\partial p}{\partial y}+\delta^2\frac{\partial \tau_{yx}}{\partial x}+\delta^2\frac{\partial \tau_{yy}}{\partial y}-\delta^2\frac{1}{D_a}v_3\,, \quad (4.13)$$

$$Re\delta\left(v_1\frac{\partial \theta}{\partial x}+v_3\frac{\partial \theta}{\partial y}\right)=\frac{1}{Pr}\left(\delta^2\frac{\partial^2\theta}{\partial x^2}+\frac{\partial^2\theta}{\partial y^2}\right)+Ec\left(\delta^2\frac{\partial v_1}{\partial x}(\tau_{xx})+\frac{\partial v_1}{\partial y}(\tau_{xy})+\delta^2\frac{\partial v_3}{\partial x}(\tau_{yx})+\delta^2\frac{\partial v_3}{\partial y}(\tau_{yy})\right)-Hc\theta. \quad (4.14)$$

The components of extra stress tensor are

$$\tau_{xx}=\frac{2}{1+\lambda_1}\left(1+\lambda_2\frac{\delta s}{d}\left(v_1\frac{\partial}{\partial x}+v_3\frac{\partial}{\partial y}\right)\right)\frac{\partial}{\partial x}(v_1+1), \quad (4.15)$$

$$\tau_{xy}=\frac{1}{1+\lambda_1}\left(1+\lambda_2\frac{\delta s}{d}\left(v_1\frac{\partial}{\partial x}+v_3\frac{\partial}{\partial y}\right)\right)\left(\frac{\partial}{\partial y}(v_1+1)+\delta^2\frac{\partial v_3}{\partial x}\right), \quad (4.16)$$

$$\tau_{yy}=\frac{2}{1+\lambda_1}\left(1+\lambda_2\frac{\delta s}{d}\left(v_1\frac{\partial}{\partial x}+v_3\frac{\partial}{\partial y}\right)\right)\frac{\partial v_3}{\partial y}. \quad (4.17)$$

By assuming wavelength is too small ($\delta \ll 1$) and applying lubrication approach we get

$$-\frac{\rho {d_1}^2}{\mu}\Omega(v_1+1)=-\frac{\partial p}{\partial x}+\frac{\partial \tau_{xy}}{\partial y}-\left(Me^2+\frac{1}{Da}\right)(v_1+1), \quad (4.18)$$

$$-\frac{\partial p}{\partial y}=0, \quad (4.19)$$

$$\frac{1}{Pr}\frac{\partial^2\theta}{\partial y^2}+Ec\tau_{xy}\left(\frac{\partial v_1}{\partial y}\right)-Hc\theta=0, \quad (4.20)$$

$$\tau_{xy}=\frac{1}{1+\lambda_1}\left(\frac{\partial}{\partial y}(v_1+1)\right). \quad (4.21)$$

The corresponding boundary conditions are

$$v_1\pm\beta\frac{\partial v_1}{\partial y}=0, \qquad at \qquad y=\pm\eta,$$

$$\theta = 0, \qquad at \qquad y = -\eta,$$

$$\theta = 1, \qquad at \qquad y = \eta. \tag{4.22}$$

## 4.3 Result and Discussions

In this section, using NDSolve command in MATHEMATICA programming language, graphs were created to illustrate how various parameters influence the temperature, velocity and streamlines structures. Figures $4.1 - 4.5$ depict the effects of rotation parameter, slip parameter, magnetic parameter, porosity parameter and relaxation parameter on velocity distribution. Figures $4.6 - 4.12$ illustrate how the temperature is affected by these parameters along with heat source parameter and Eckert number. One of the most important phenomena frequently seen in the peristaltic flows, porous media or MHD flow is trapping, by which streamlines form closed loops or recirculating zones. The conduct of different factors on streamline structures is depicted in figures $4.13 -$ 4.17.

The velocity variation for various rotation parameter values can be seen in figure 4.1. Coriolis forces are introduced as the rotation parameter rises, altering the fluid's momentum distribution which leads to higher velocity in the channel. Figure 4.2 displays the velocity fluctuation with respect to the slip parameter $\beta$. A greater slip parameter results in less friction near the wall. As $\beta$ rises, fluid flows more quickly throughout, particularly in the center. Figure 4.3 plots velocity variation with respect to varying magnetic parameter values. When a magnetic field is applied, the Lorentz force is produced which opposes the motion of the fluid. Consequently, velocity falls across the domain as the magnetic parameter $Me$ rises.

The velocity variation for various porosity parameter values can be seen in figure 4.4. Increase in the porosity parameter $Da$ cause the porous medium to become more flow resistive, leading to lessen the velocity. The effect of relaxation parameter on the velocity profile can be seen in figure 4.5. As the relaxation parameter $\lambda_1$ rises, the fluid's resistance to deformation enhances, which causes resistance in the flow of fluid. Thus, velocity decreases as $\lambda_1$ rises.

Figure 4.6 depicts how the temperature changes with varying values of rotation parameter $\Omega$. As the rotation parameter $\Omega$ rises, the rotational effect promotes stronger mixing, pushing heat away

and the temperature falls throughout the flow domain. The variation in temperature with regard to the slip parameter is plotted in figure 4.7. Friction is reduced at the boundary when slip parameter increases and fluid movement improves. Consequently, declining heat diffusion causing decline in temperature throughout. The temperature fluctuations relative to the magnetic parameter is depicted in figure 4.8. As the magnetic parameter rises, a greater magnetic field is applied, suppressing fluid motion due to Lorentz force which increases the thickness of thermal boundary layer. The temperature profile shifts upward, indicating an increase in temperature.

The temperature profile can be seen in figure 4.9 for various values of relaxation parameter $\lambda_1$. Heat builds up more in the medium with an increased $\lambda_1$ because the heat flux reacts to temperature gradient more slowly which leads to higher temperature profile. Figure 4.10 plots the temperature changes for various porosity parameter values. The temperature rises as porosity parameter $Da$ increases because heat transmission improves as fluid moves more freely. The temperature distribution is depicted in figure 4.11 with respect to various values of the heat source parameter. More thermal energy is produced inside the fluid as $Hc$ rises resulting in less cooling and more heat accumulation. Consequently, the overall temperature rises. The temperature change for various Eckert number values can be seen in figure 4.12. Because of improved viscous dissipation, the temperature rises as $Ec$ rises and the curves shift upward showing higher thermal energy.

The streamline pattern of the fluid flow with the parameter value $\lambda_1 = 1$ can be seen in figure 4.13 (a). the appearance of trapped bolus regions is demonstrated by the presence of closed streamlines. The two separate boluses shown in the domain imply that the flow permits entrapment, which lowers net transport and increases internal mixing. The streamline pattern of fluid flow for $\lambda_1 = 0.8$ is shown in figure 4.13 (b). the bolus region's size has decreased significantly. This drop implies that fewer particles have been trapped within the recirculating zones and that the trapping strength has reduce. The streamline pattern of fluid flow for $\lambda_1 = 1.6$ is depicted in figure 4.13 (c). the higher bolus size implies a stronger trapping effect. Now that the recirculating boluses are more prominent and enlarged, it indicates that a larger volume of fluid is confined inside the vortical structure. Figure 4.14 (a) shows the streamline structure of fluid flow for $Da = 0.01$, representing extremely low permeability porous medium. Trapping phenomena are weaker and bolus regions are substantially smaller and more densely packed suggesting that fewer fluid particles are being trapped in recirculation zones. fluid streamline pattern for $Da = 0.1$ can be seen in figure 4.14 (b). Reduced trapping is demonstrated by moderate bolus size, compact streamlines, smaller recirculation zones. figure 4.14 (c) depicts the fluid streamline pattern for $Da = 0.2$, showing higher

permeability. Because to improved fluid mobility, bolus increases as Da rises. The recirculating regions have enlarged, suggesting stronger trapping and more intense internal fluid movement.

Figure 4.15 (a) plots the streamline pattern of the fluid flow for $Me$ = 0.01, exhibiting a very weak influence of magnetic field. The bolus size is comparatively large and well-defined, indicating strong trapping. figure 4.15 (b) illustrates the streamline configuration of fluid flow for $Me$ = 1, which shows reduction in trapping strength. As $Me$ increases to 1, due to suppressed fluid mobility bolus size decreases and trapping effect weakens, which lessens the extent of recirculation. In figure 4.15 (c), the streamline structure of the fluid flow for $Me$ = 2 can be seen, indicating that bolus region has contracted and become more compressed. Consequently, trapping effect is decreased. Figure 4.16 (a) displays the streamline pattern of the fluid flow when $\beta$ = 0, which represents the neutral or initial trapping state. trapping is clearly associated with symmetric bolus formation, where fluid particles circulate in confined zones and bolus size is moderate which is a baseline scenario. The fluid streamline pattern for $\beta$ = 0.2, indicating improved internal circulation can be seen in Figure 4.16 (b). Stronger trapping behaviour with clearly defined closed loops is reflected by slightly larger and more prominent bolus regions. Figure 4.16 (c) depicts fluid streamlines structure for $\beta$ = 0.4, indicating increased recirculatory motion. Bolus size has increased with increasing $\beta$ and trapping becomes more apparent and stronger. The fluid streamline distribution for $\Omega$ = 0.01 is depicted in figure 4.17 (a), which indicate strong trapping phenomena. The symmetric and large bolus structure indicate that the fluid particles are effectively circulating within trapped zones without significant distortion. Figure 4.17 (b) illustrates the streamline configuration for $\Omega$ = 0.1. The bolus structure appears slightly compressed and shifted suggesting reduced recirculation, demonstrating the effect of increased rotation. Figure 4.17 (c) displays the fluid streamline structure for $\Omega$ = 0.2. As $\Omega$ increases, bolus formation decreases as a consequence of rational forces suppressing symmetric recirculation and weakening trapping behaviour.

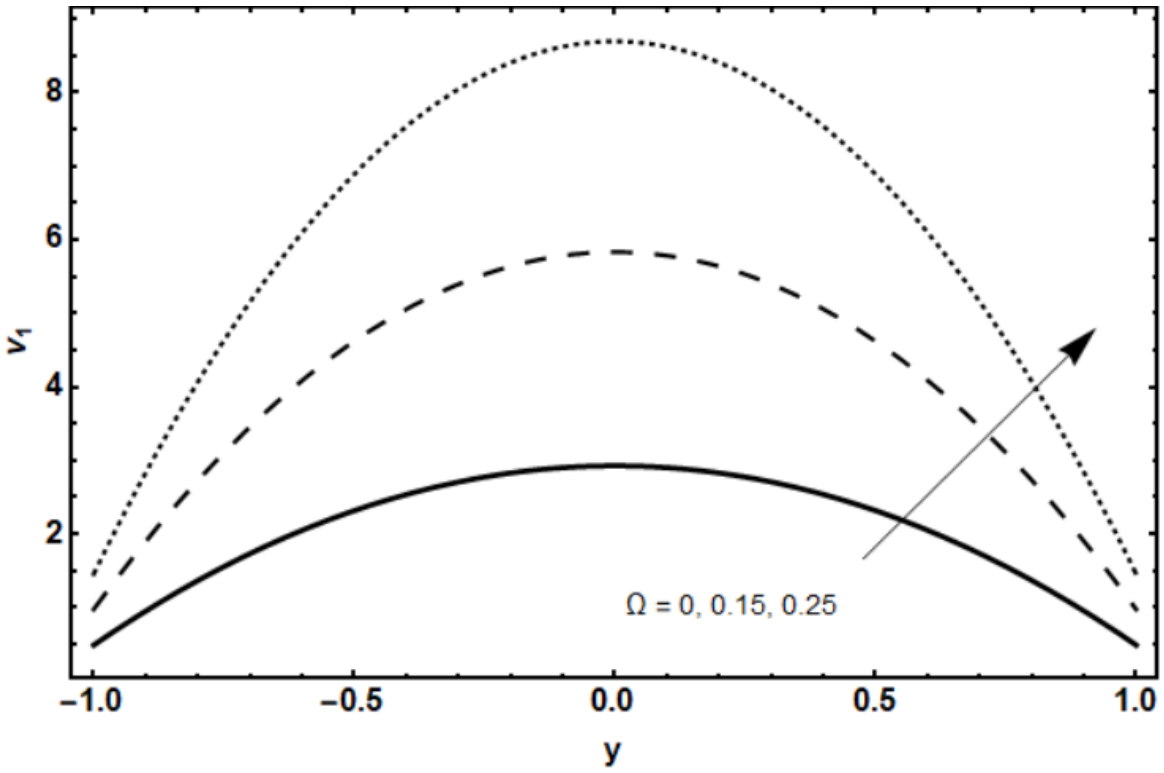


**Figure 4.1** Velocity variation for the rotation parameter.

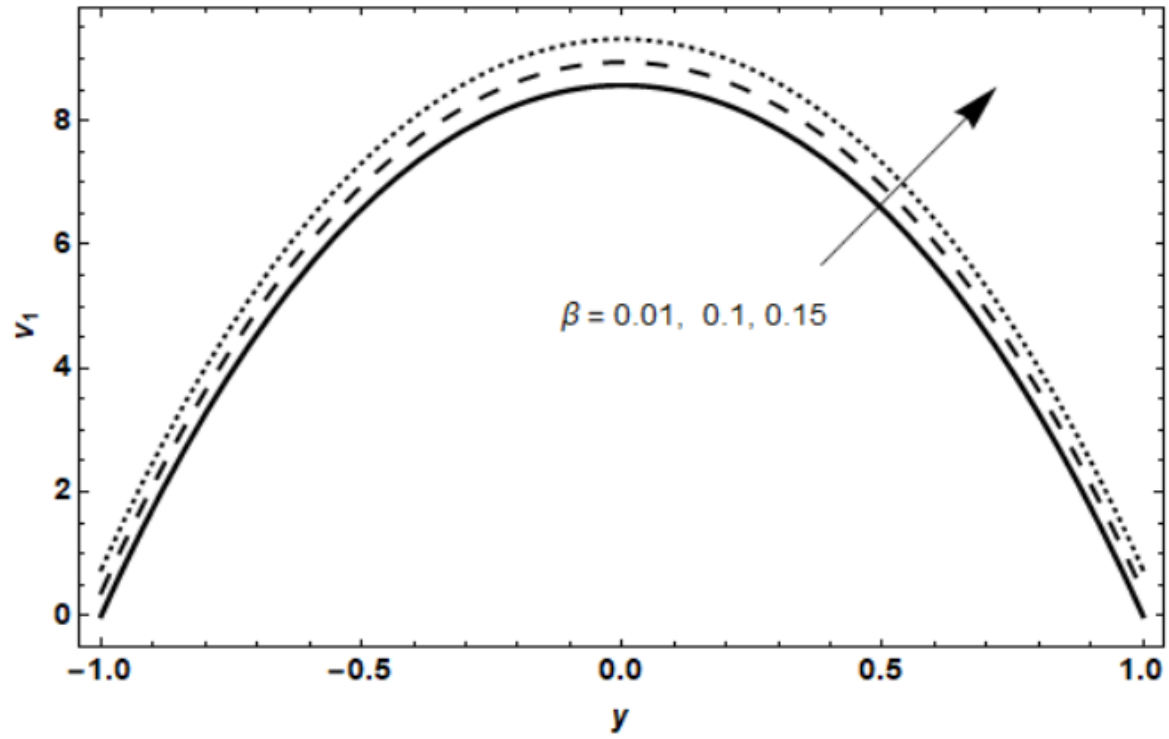


**Figure 4.2** Velocity variation for the Slip Parameter.

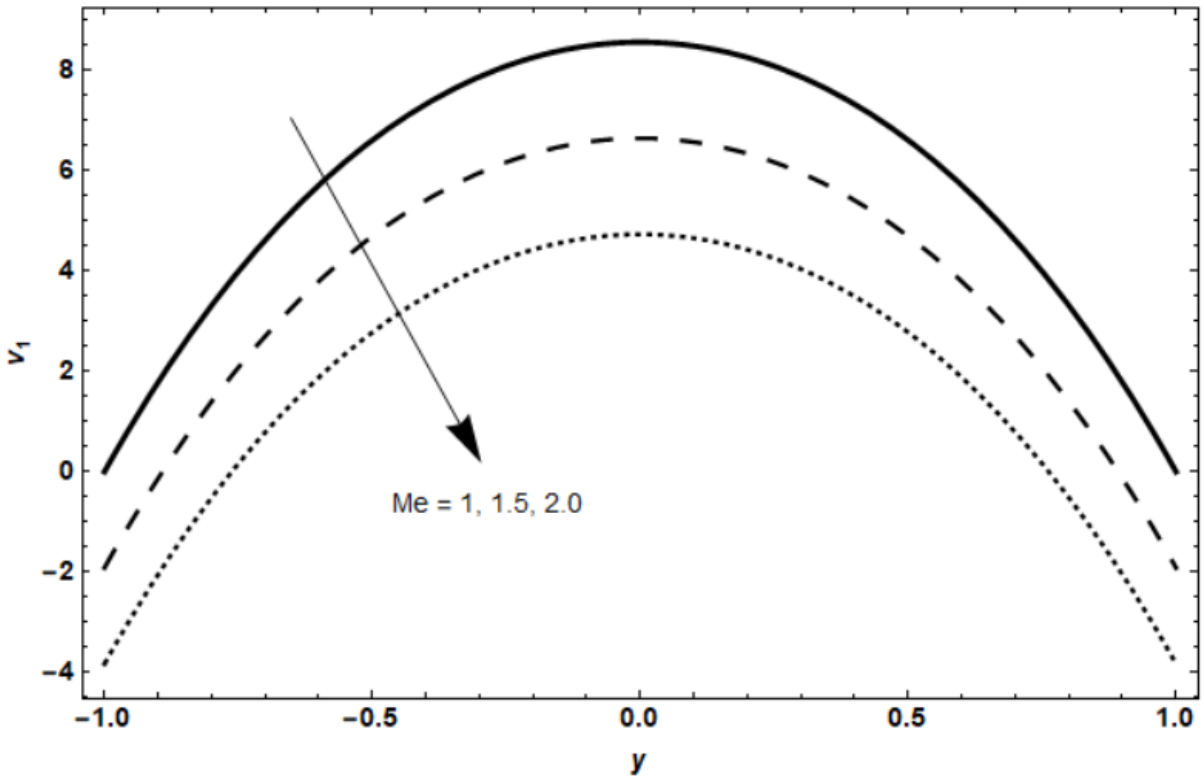


**Figure 4.3** Velocity variation for the magnetic parameter.

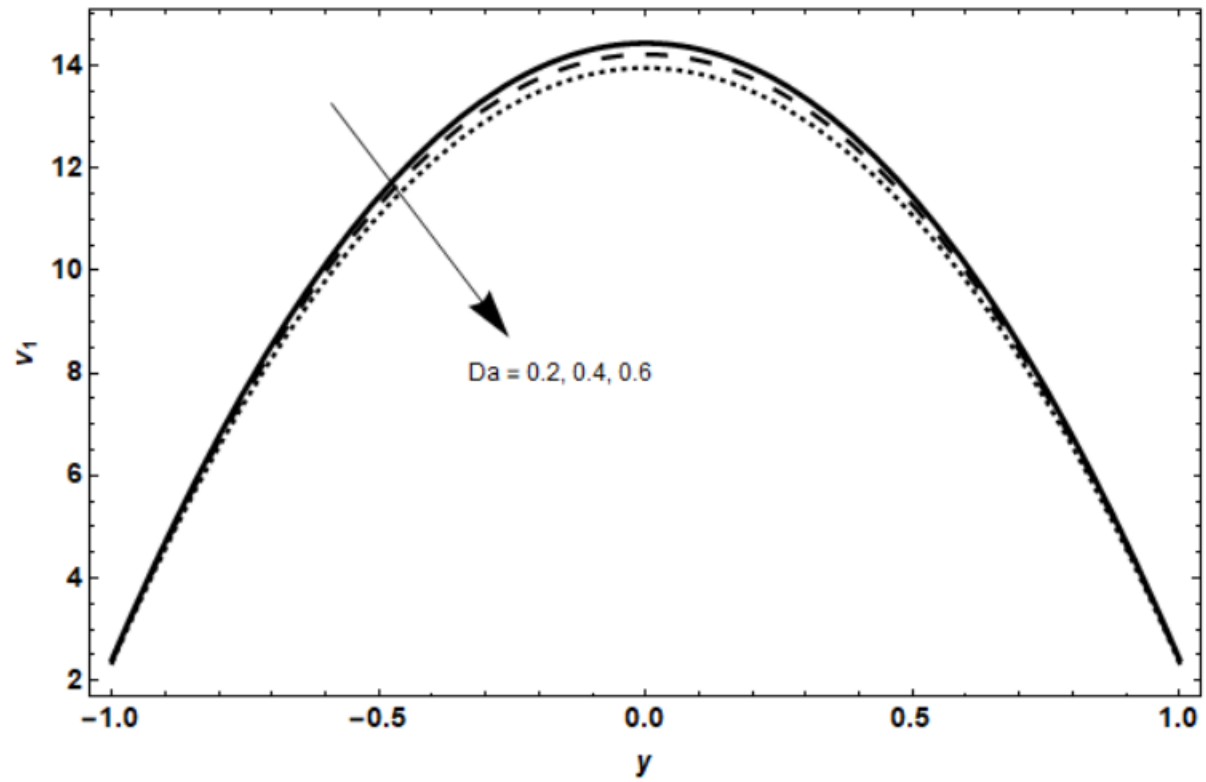


**Figure 4.4** Velocity variation for the porosity parameter.

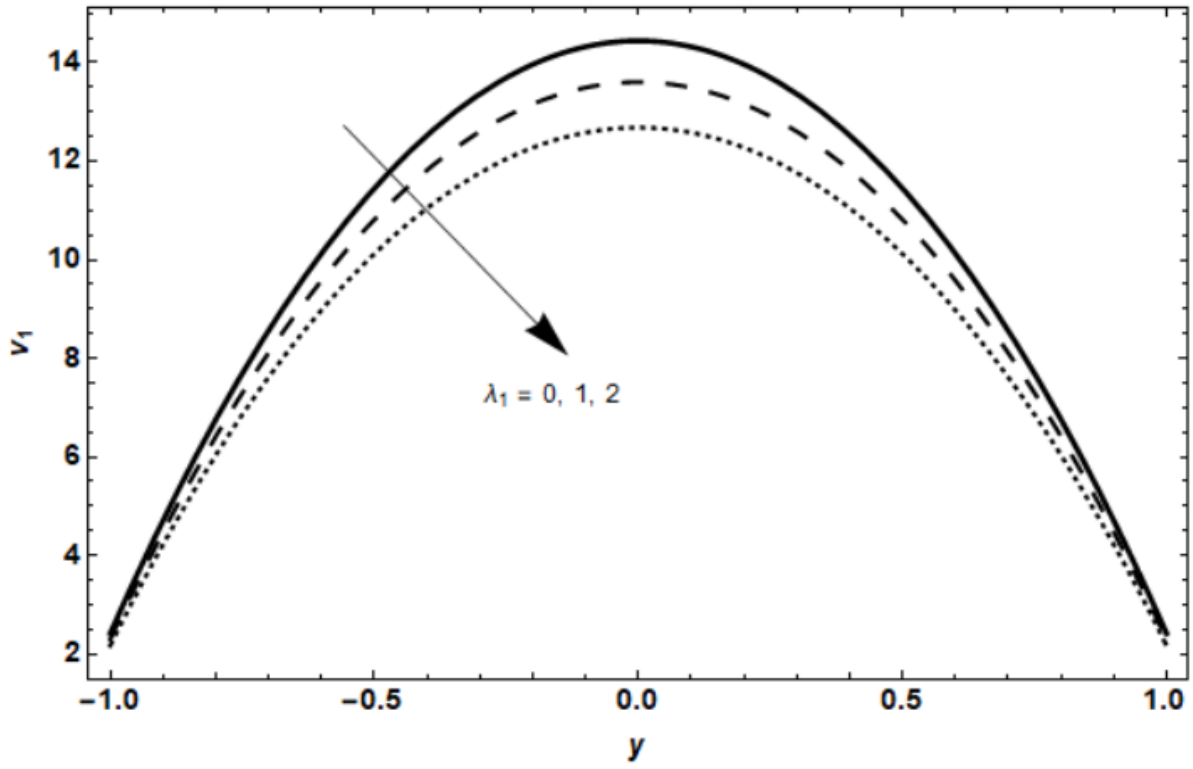


**Figure 4.5** Velocity variation for the Relaxation parameter.

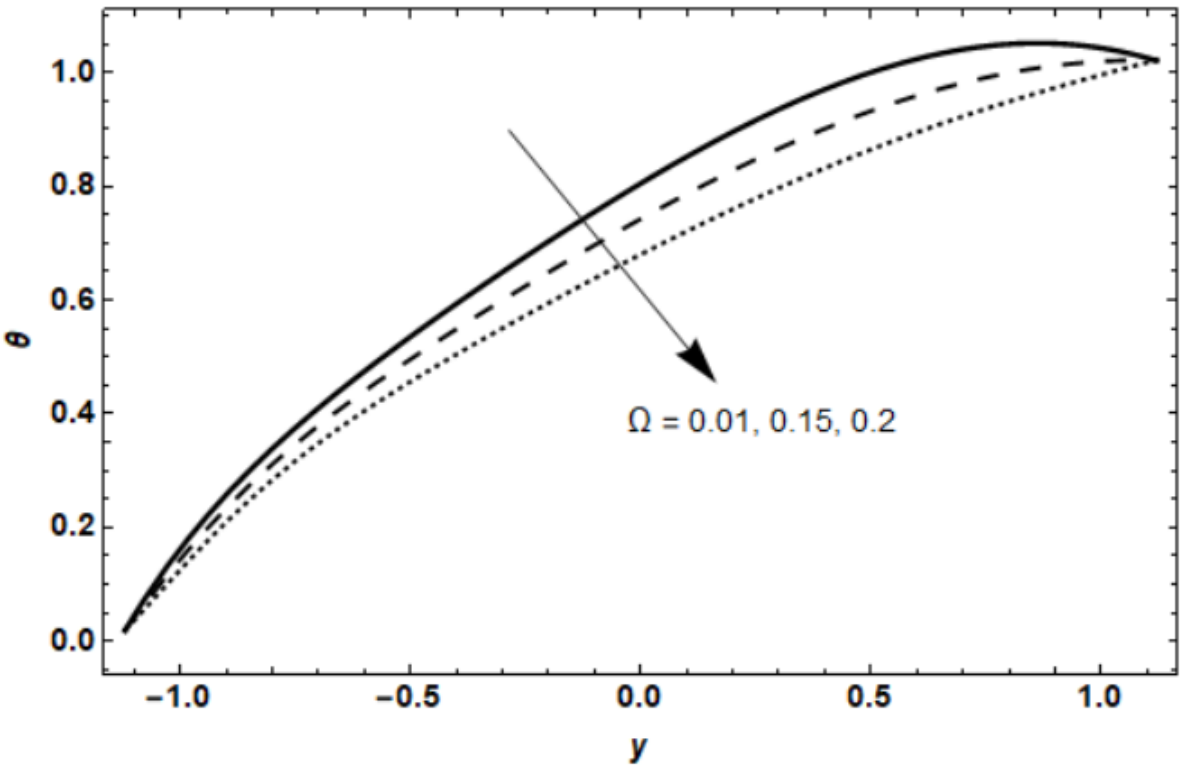


**Figure 4.6** Temperature variation for the rotation parameter.

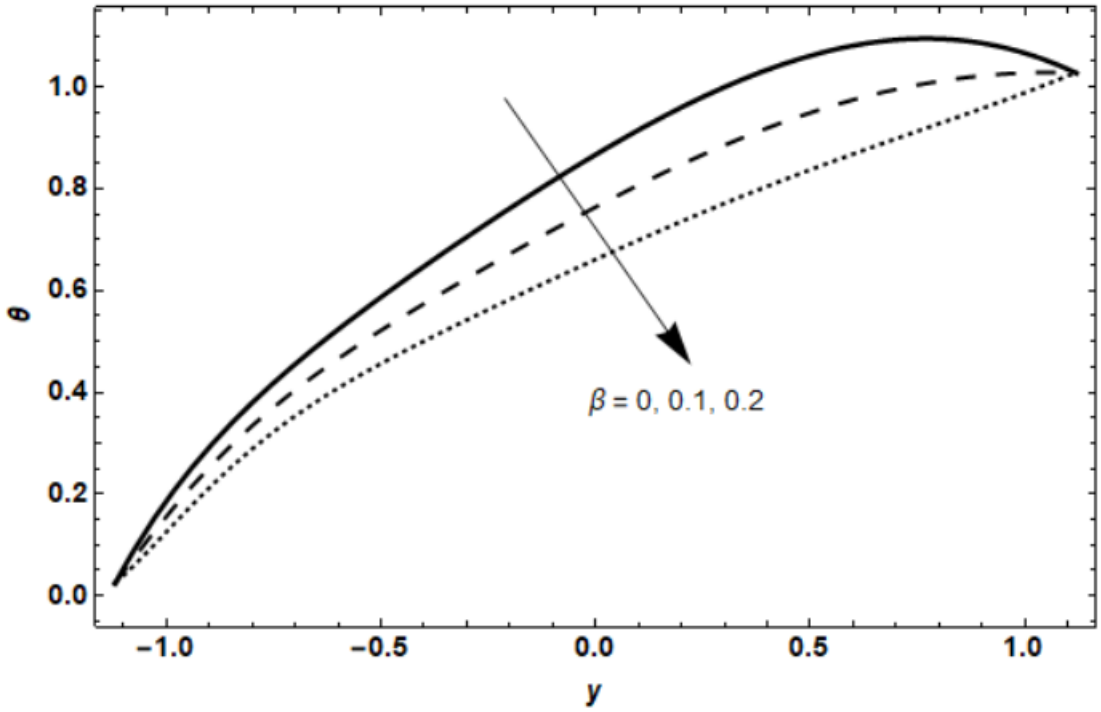


**Figure 4.7** Temperature variation for the slip parameter.

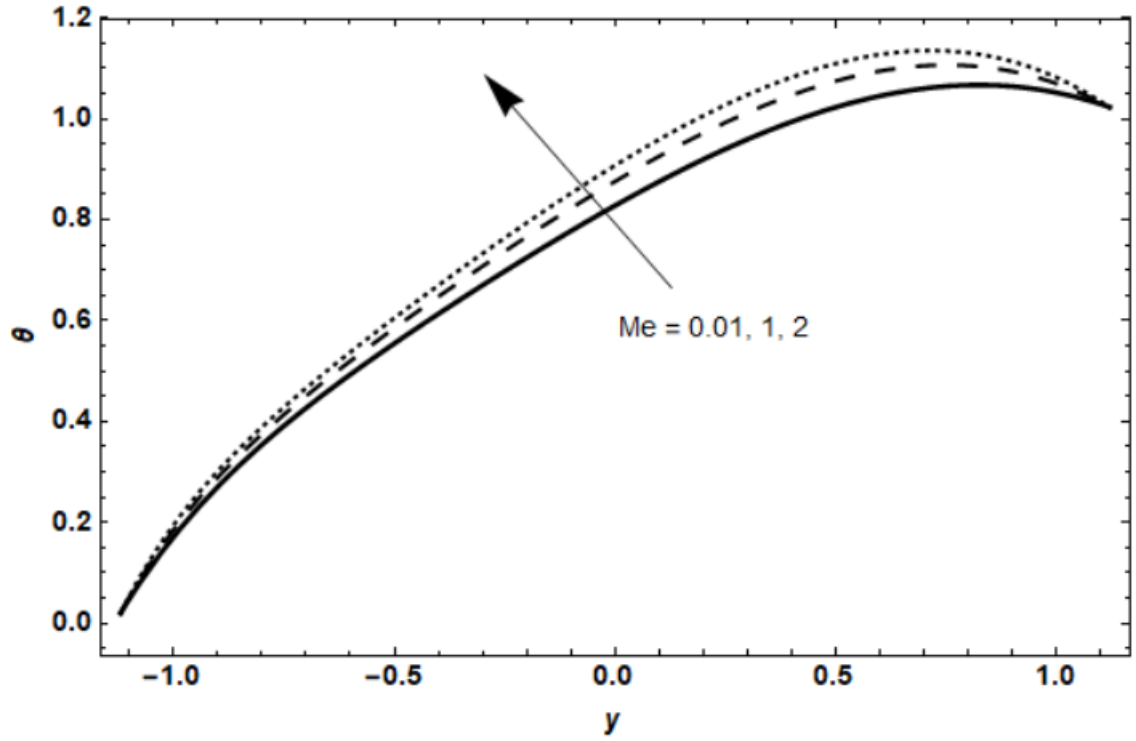


**Figure 4.8** Temperature variation for the magnetic parameter.

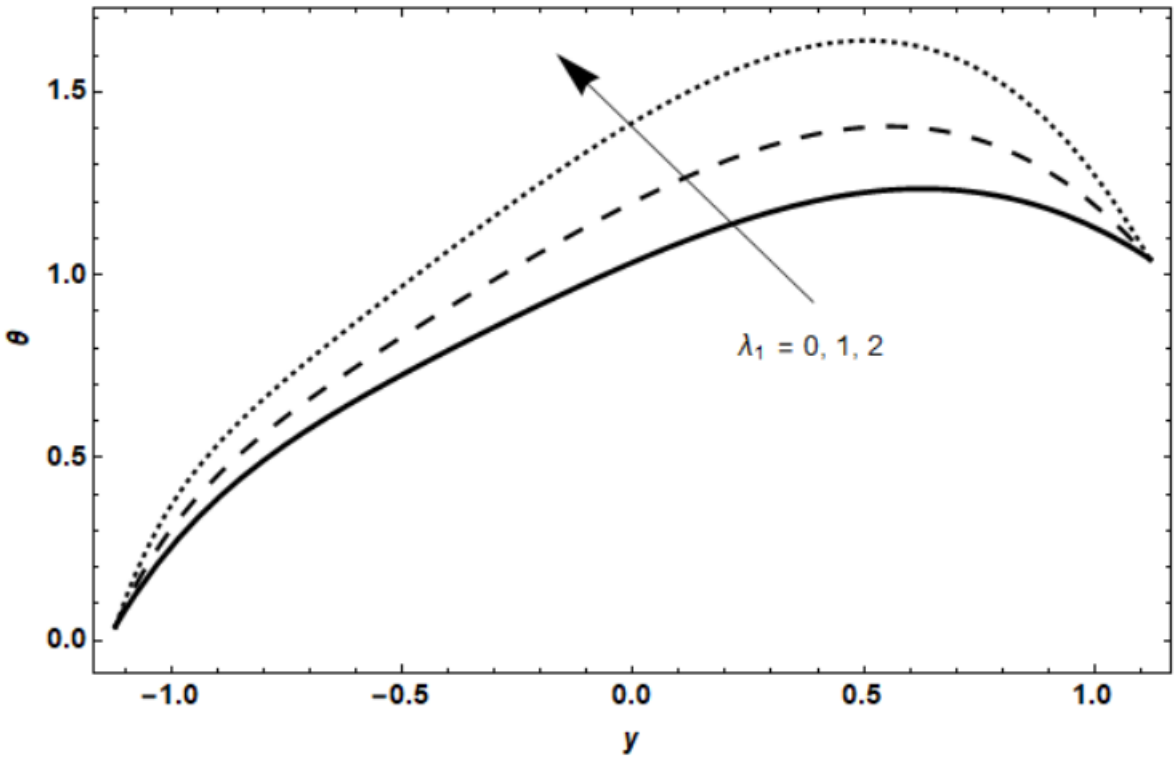


**Figure 4.9** Temperature variation for the relaxation parameter.

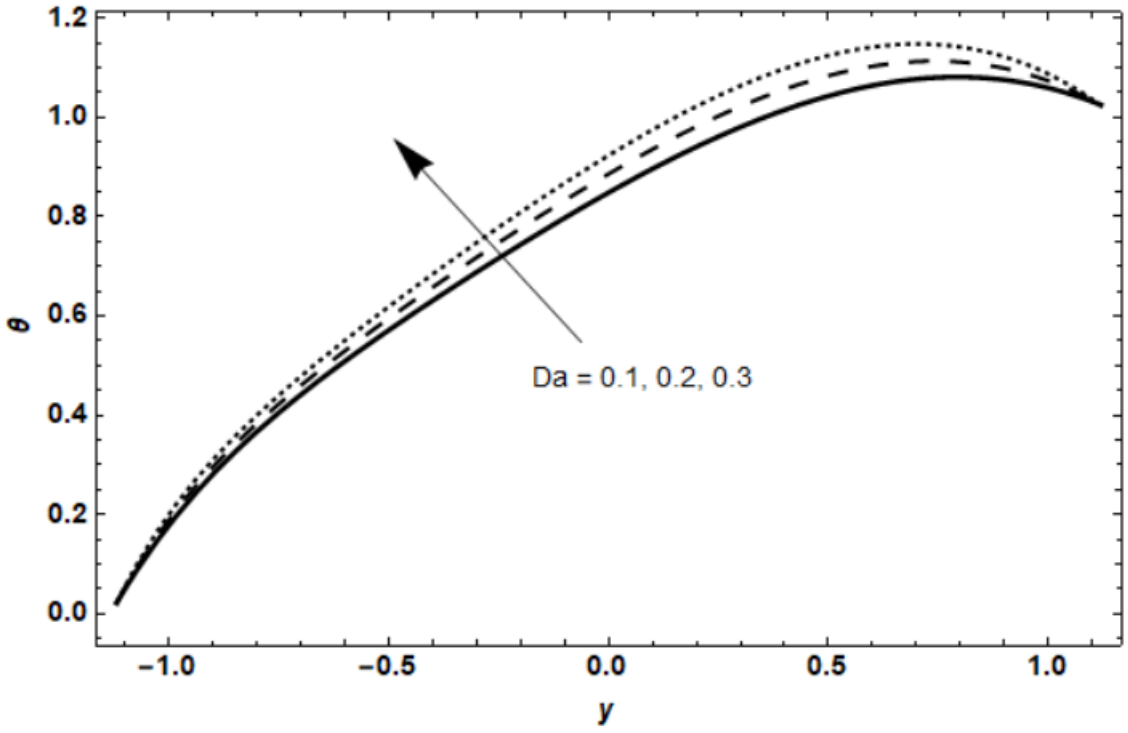


**Figure 4.10** Temperature variation for the porosity parameter.

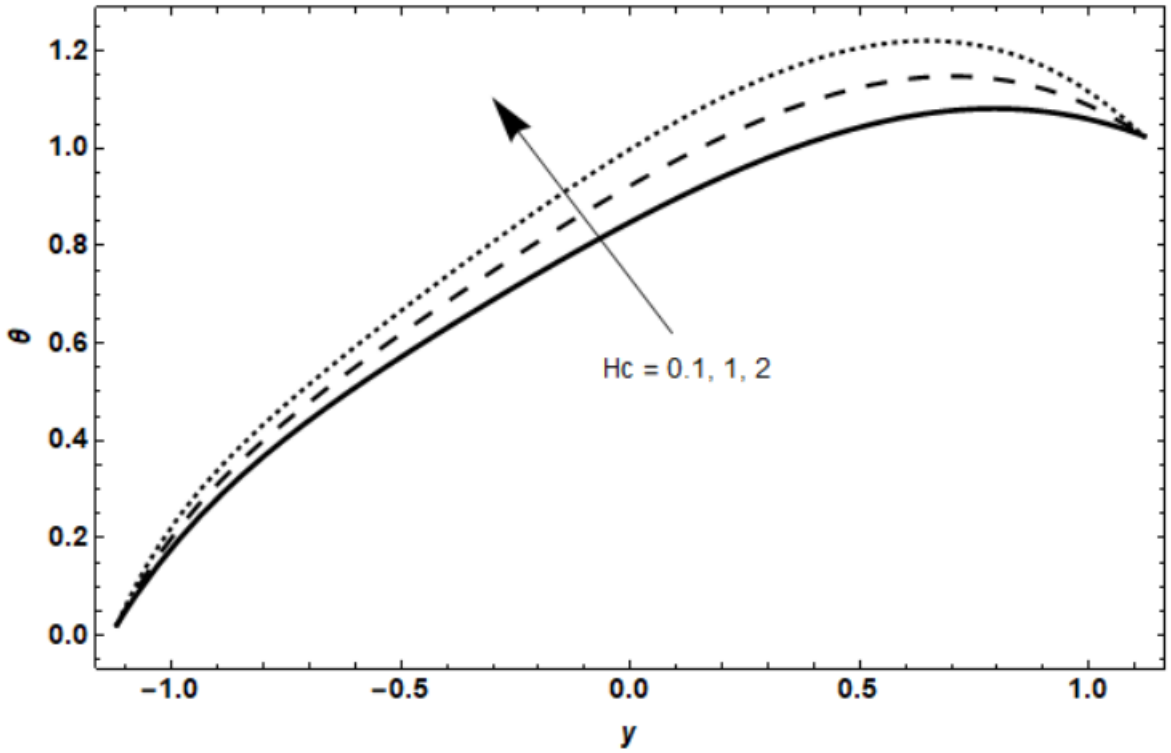


**Figure 4.11** Temperature variation for the heat source parameter.

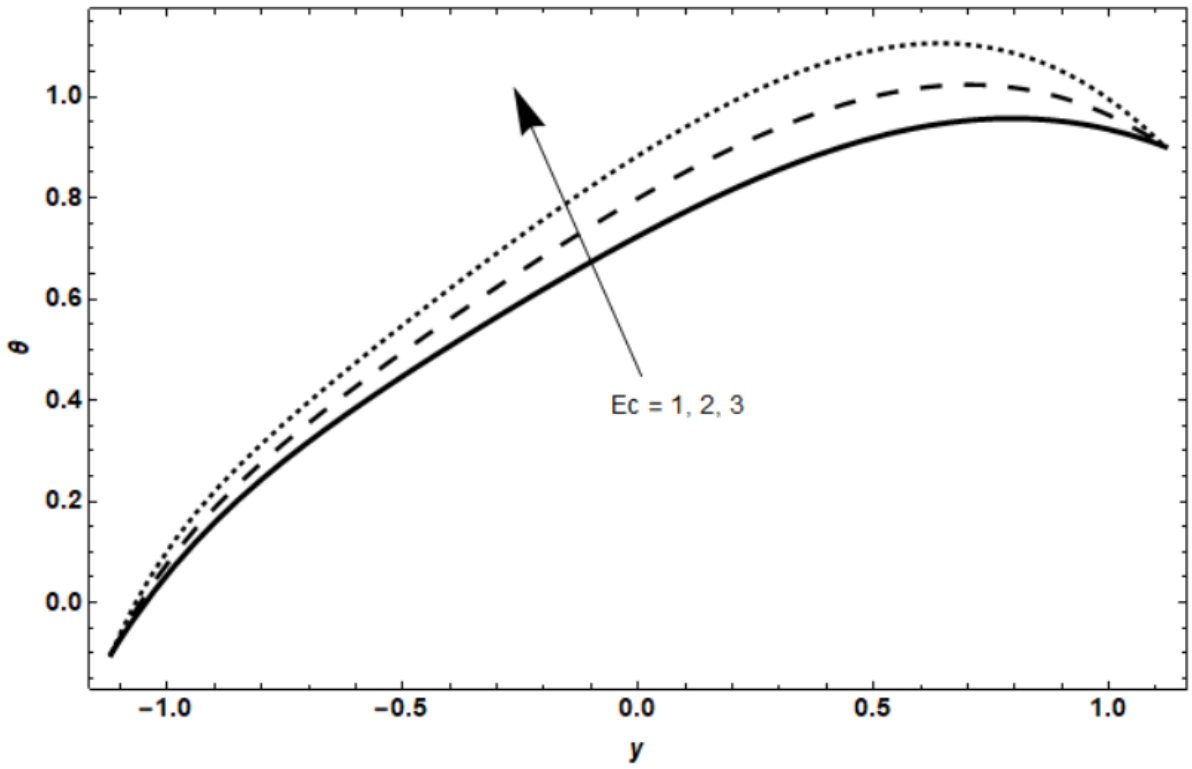


**Figure 4.12** Temperature variation for the Eckert number.

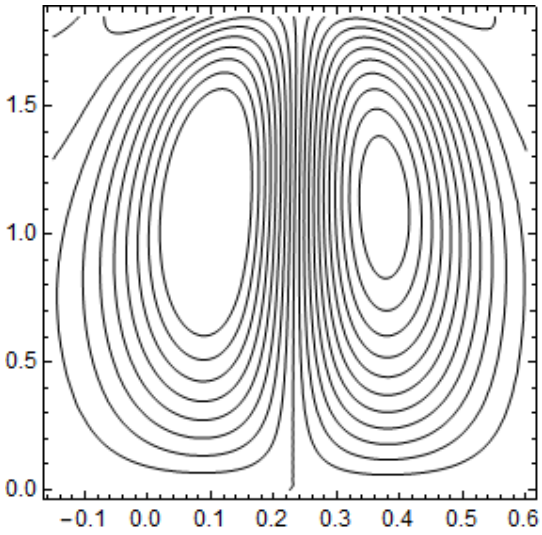


(a) $\lambda_1 = 0$

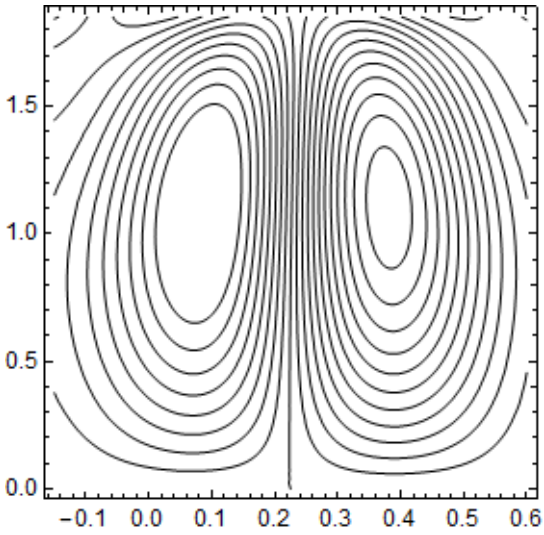


(b) $\lambda_1 = 0.8$

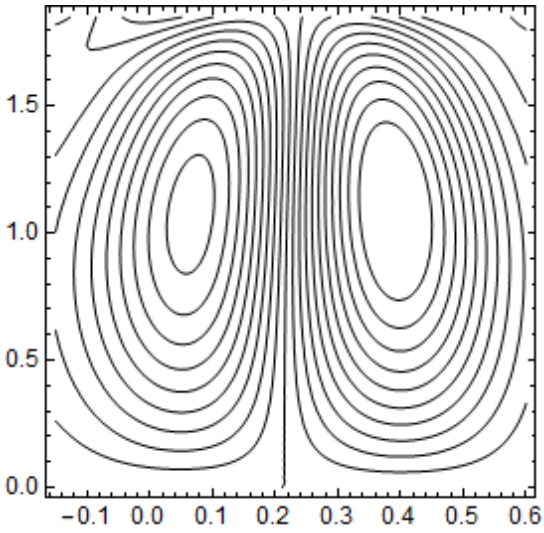


(c) $\lambda_1 = 1.6$

**Figure 4.13** depicts the significance of $\lambda_1$ on the fluid streamline structures

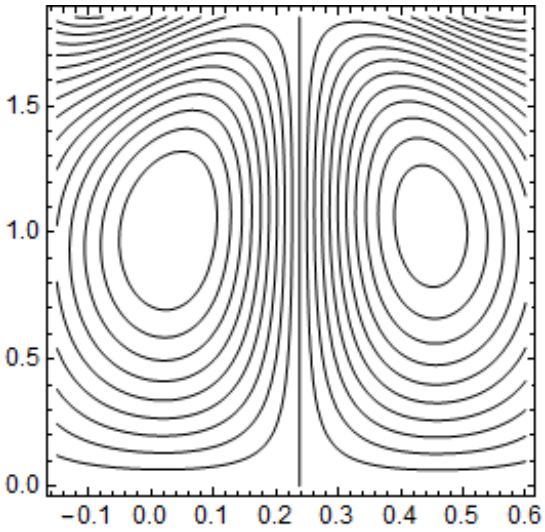


(a) $Da = 0.01$

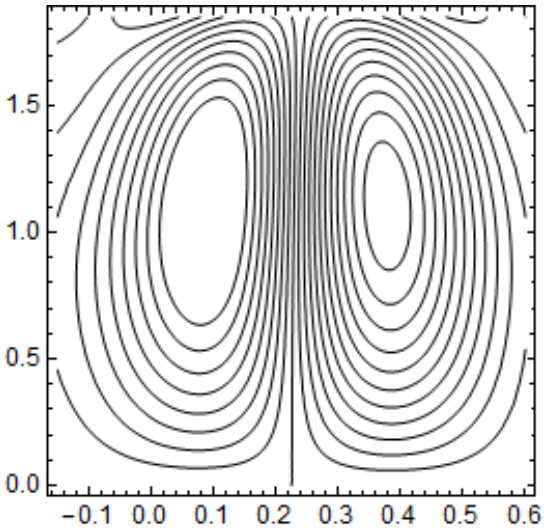


(b) $Da = 0.1$

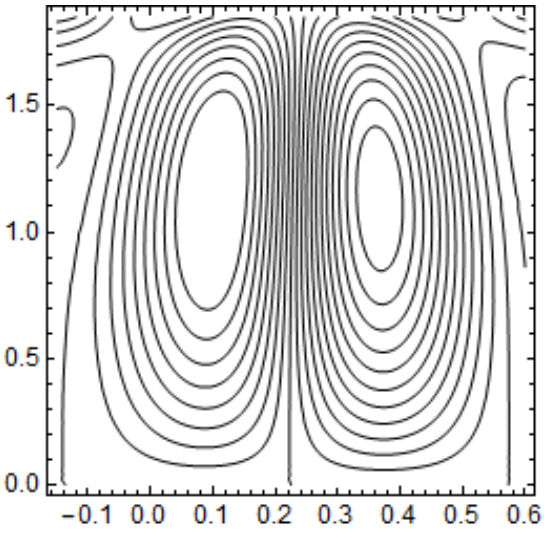


(c) $Da = 0.2$

**Figure 4.14** depicts the significance of $Da$ on the fluid streamline structures

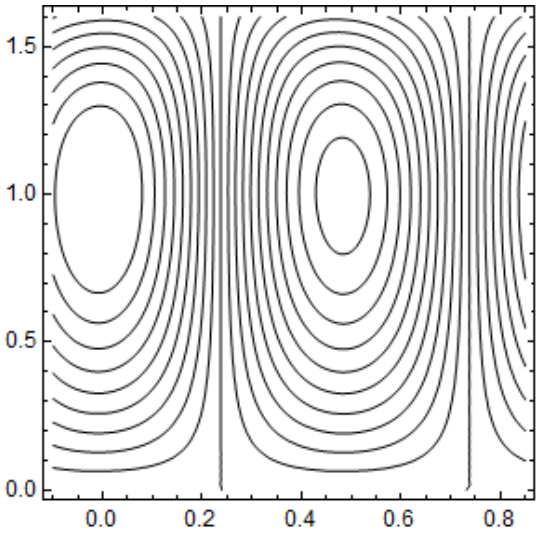


(a) $Me = 0.01$

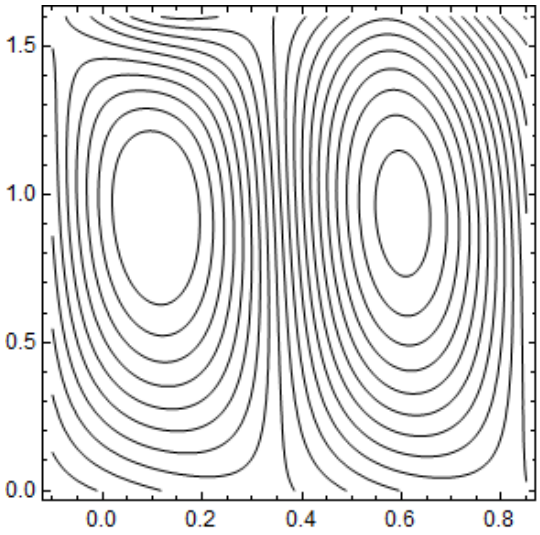


(b) $Me = 1$

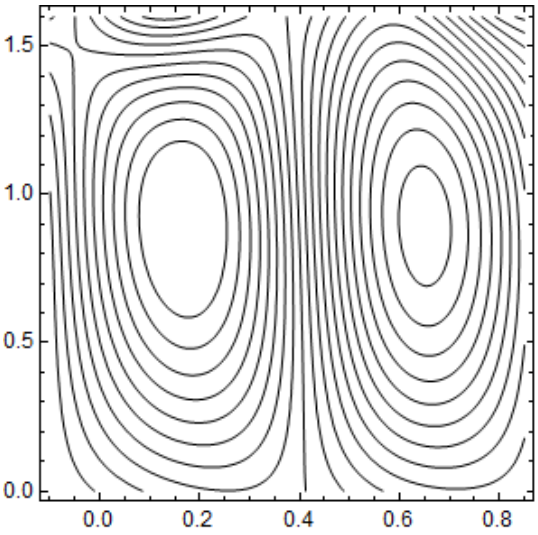


(c) $Me = 2$

**Figure 4.15** depicts the significance of $Me$ on the streamline structures

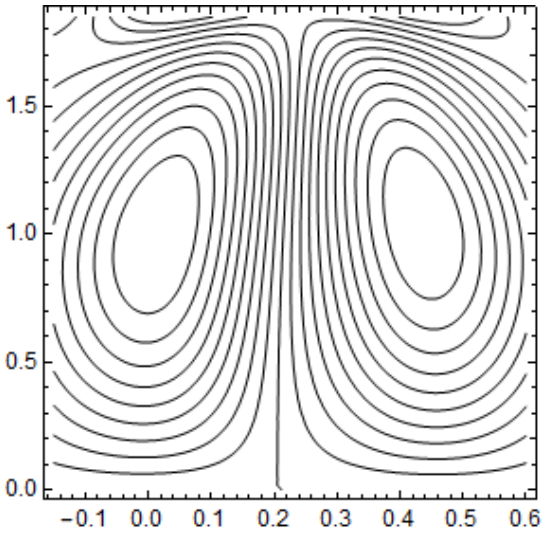


(a) $\beta = 0$

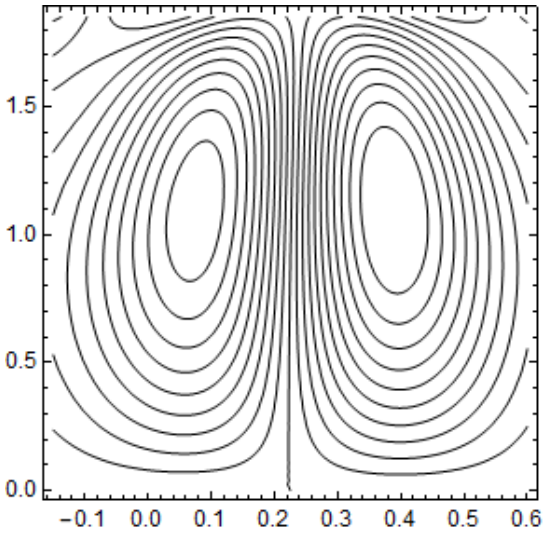


(b) $\beta = 0.2$

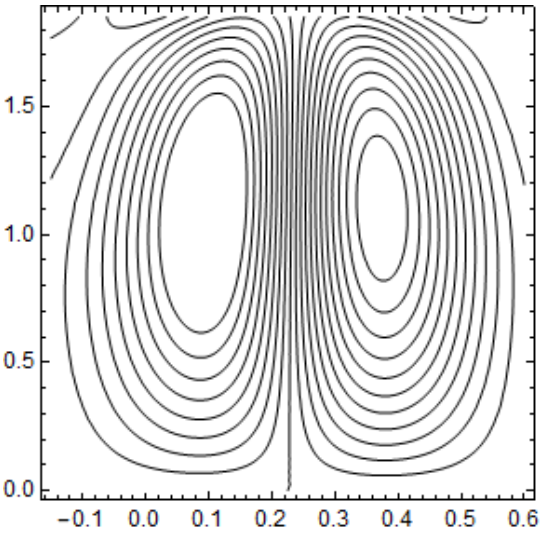


$(c)\ \beta = 0.4$

**Figure 4.16** depicts the significance of $\beta$ on the fluid streamline structures

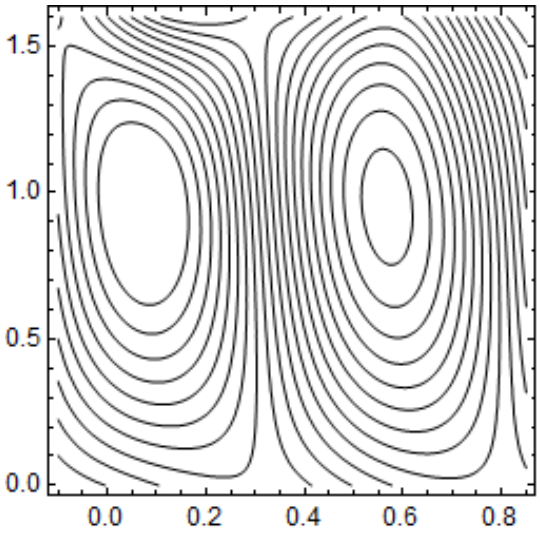


(a) $\Omega = 0.01$

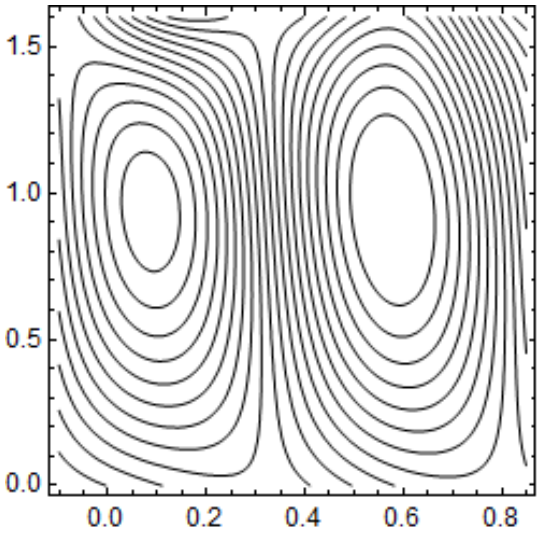


(b) $\Omega = 0.1$

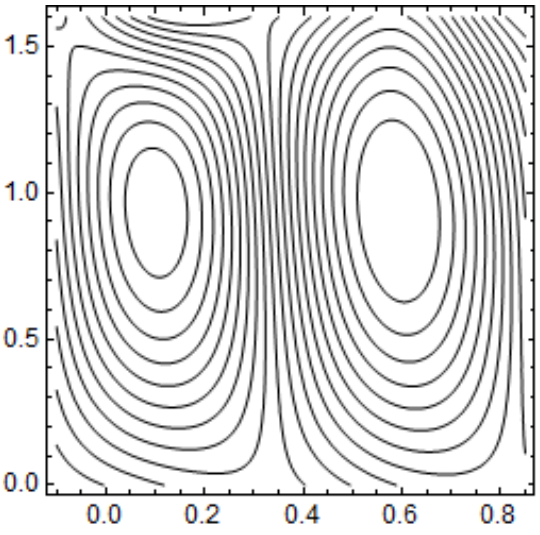


(c) $\Omega = 0.2$

**Figure 4.17** depicts the significance of $\Omega$ on the streamline structures

# CHAPTER 5

# CONCLUSION AND FUTURE WORK

## 5.1 Conclusion

The purpose of this study is to investigates the impact of rotation on a non-Newtonian Jeffrey fluid's temperature and magnetohydrodynamic peristaltic flow in a porous medium. Considering low Reynolds number and long wavelength, the numerical method is employed. Through In-depth stimulations and graphical analysis with Mathematica, this study focuses on the impact of various parameters on streamline structures, velocity and temperature distribution. The findings indicates that these parameters have a significant effect on fluid's thermal characteristics and flow behavior.

The results demonstrate that the considerable increase in fluid velocity is caused by the rotation parameter $\Omega$ and slip parameter $\beta$. The porosity parameter $Da$, relaxation parameter $\lambda_1$ and the magnetic parameter $Me$ resists fluid motion and reduces velocity throughout the domain.

It is also observed that the temperature profile rises with higher values of the parameters including magnetic parameter $Me$, relaxation parameter $\lambda_1$ , porosity parameter $Da$, heat source parameter $Hc$ and Eckert number $Ec$. A decline is observed in the temperature with enhancement in the rotation and slip parameter. Additionally, internal heat production by $Hc$ and viscous dissipation through $Ec$ substantially raise fluid temperature.

Trapping is an important mechanism to be study in the peristaltic flow of the fluids. In this study, trapping effect is influenced by relaxation parameter $\lambda_1$, porosity parameter $Da$ and slip parameter $\beta$, with higher values resulting in stronger trapping behavior and larger bolus. While an increase in magnetic parameter $Me$ and rotation parameter $\Omega$, bolus formation decreases and results in weak trapping behavior.

## 5.2 Future Work

In this suggested study, MHD and porosity is incorporated in the symmetric channel along with rotation phenomena. The fluid model considered is Jeffrey model that provides an insight to keenly investigate the time taken by the fluid to get back to its original position after disturbance. This

suggested model has still much to explore.

- This model can be broadened by incorporating more complex boundary conditions, additional factors or using different fluid models instead of Jeffrey fluid.
- Using nanoparticles to investigate peristaltic nanofluid flow could provide further insights of heat transmission.
- Various numerical methods such as finite difference or finite element may also be employed for solving governing equations instead of utilizing perturbation techniques which allows the study of higher Reynolds number and shorter wavelength.
- Furthermore, the practical applicability of model in many applications such as biomedical engineering, industrial processes and petroleum engineering would be enhanced by experimental validation of the theoretical conclusions.

## References


Abbas, Z., & Hayat, T. (2008). Radiation effects on MHD flow in a porous space. *International Journal of Heat and Mass Transfer*, *51*(5-6), 1024-1033.

Abd-Alla, A., Abo-Dahab, S., Salah, D. M., Bayones, F., & Abdelhafez, M. (2023). Magneto-hydrodynamic peristaltic flow of a Jeffery fluid in the presence of heat transfer through a porous medium in an asymmetric channel. *Scientific Reports*, *13*(1), 21088.

Abd-Alla, A., Abo-Dahab, S., Thabet, E. N., Bayones, F., & Abdelhafez, M. (2023). Heat and mass transfer in a peristaltic rotating frame Jeffrey fluid via porous medium with chemical reaction and wall properties. *Alexandria Engineering Journal*, *66*, 405-420.

Al-Khafajy, D. G. S., Lelo, A. K., & Shallal, E. A. (2021). Influence of heat carry on magnetohydrodynamics oscillatory flow for variable viscosity Carreau fluid through a porous medium. *Journal of Interdisciplinary Mathematics*, *24*(3), 519-535.

Ayub, R., Ahmad, S., & Ahmad, M. (2022). MHD rotational flow of viscous fluid past a vertical plate with slip and Hall effect through porous media: A theoretical modeling with heat and mass transfer. *Advances in Mechanical Engineering*, *14*(6), 16878132221103330.

Bansal, R. (2004). *A textbook of fluid mechanics and hydraulic machines*. Laxmi publications.

Barton, C., & Raynor, S. (1968). Peristaltic flow in tubes. *The Bulletin of mathematical biophysics*, *30*, 663-680.

Brown, T. D., & Hung, T.-K. (1977). Computational and experimental investigations of two-dimensional nonlinear peristaltic flows. *Journal of Fluid Mechanics*, *83*(2), 249-272.

Burns, J., & Parkes, T. (1967). Peristaltic motion. *Journal of Fluid Mechanics*, *29*(4), 731-743.

Crowell, B. (2001). *Conservation laws* (Vol. 2). Light and Matter.

Eldesoky, I. M., Nayel, M. S., Galal, A. A., & Raslan, H. M. (2020). Combined effects of space porosity and wall properties on a compressible Maxwell fluid with MHD peristalsis. *SN Applied Sciences*, *2*(12), 2118.

Ellahi, R., Bhatti, M. M., Riaz, A., & Sheikholeslami, M. (2014). Effects of magnetohydrodynamics on peristaltic flow of Jeffrey fluid in a rectangular duct through a porous medium. *Journal of Porous Media*, *17*(2).

Ellahi, R., & Hameed, M. (2012). Numerical analysis of steady non-Newtonian flows with heat transfer analysis, MHD and nonlinear slip effects. *International Journal of Numerical Methods for Heat & Fluid Flow*, *22*(1), 24-38.

Elshehawey, E., Eldabe, N. T., Elghazy, E., & Ebaid, A. (2006). Peristaltic transport in an asymmetric channel through a porous medium. *Applied Mathematics and Computation*, *182*(1), 140-150.

Farooq, S., Shoaib, T., Bukhari, S., Alqahtani, A., Malik, M., Abdullaev, S., & Alhazmi, S. (2023). Peristaltic motion of Jeffrey fluid with nonlinear mixed convection. *Heliyon*, *9*(11).

Fauci, L. J. (1992). Peristaltic pumping of solid particles. *Computers & fluids*, *21*(4), 583-598.

Granger, R. A. (2012). *Fluid mechanics*. Courier Corporation.

Gudekote, M., Choudhari, R., Sanil, P., Hadimani, B., Vaidya, H., & Prasad, K. V. (2024). MHD Effects on the Peristaltic Transport of Non-Newtonian Eyring–Powell Fluid with Heat and Mass Transfer in an Inclined Uniform Channel. *Arabian Journal for Science and Engineering*, 1-17.

Hafez, N., Abd-Alla, A., & Metwaly, T. (2023). Influences of rotation and mass and heat transfer on MHD peristaltic transport of Casson fluid through inclined plane. *Alexandria Engineering Journal*, *68*, 665-692.

Hayat, T., & Ali, N. (2008). Peristaltic motion of a Jeffrey fluid under the effect of a magnetic field in a tube. *Communications in Nonlinear Science and Numerical Simulation*, *13*(7), 1343-1352.

Hayat, T., Ali, N., Asghar, S., & Siddiqui, A. M. (2006). Exact peristaltic flow in tubes with an endoscope. *Applied Mathematics and Computation*, *182*(1), 359-368.

Javid, K., Asghar, Z., Saeed, U., & Waqas, M. (2022). Porosity effects on the peristaltic flow of biological fluid in a complex wavy channel. *Pramana*, *96*(1), 2.

Jawad, Q. K., & Abdulhadi, A. M. (2023). Influence of MHD and Porous Media on Peristaltic Transport for Nanofluids in An Asymmetric Channel. *Iraqi Journal of Science*, 1344-1360.

Jyothi, K. L., Devaki, P., & Sreenadh, S. (2013). Pulsatile flow of a Jeffrey fluid in a circular tube having internal porous lining. *International Journal of Mathematical Archive*, *4*(5), 75-82.

Kasaeian, A., Daneshazarian, R., Mahian, O., Kolsi, L., Chamkha, A. J., Wongwises, S., & Pop, I. (2017). Nanofluid flow and heat transfer in porous media: a review of the latest developments. *International Journal of Heat and Mass Transfer*, *107*, 778-791.

Khan, A., & Rafaqat, R. (2021). Effects of radiation and MHD on compressible Jeffrey fluid with peristalsis. *Journal of Thermal Analysis and Calorimetry*, *143*, 2775-2787.

Kothandapani, M., & Srinivas, S. (2008). Peristaltic transport of a Jeffrey fluid under the effect of magnetic field in an asymmetric channel. *International Journal of Non-Linear Mechanics*, *43*(9), 915-924.

Kumar, B. R., & Naidu, K. (1995). A numerical study of peristaltic flows. *Computers & fluids*, *24*(2), 161-176.

Kundu, P. K., Cohen, I. M., Dowling, D. R., & Capecelatro, J. (2024). *Fluid mechanics*. Elsevier.

Latham, T. W. (1966). *Fluid motions in a peristaltic pump* Massachusetts Institute of Technology].

Mahmoud, S. R. (2011). Effect of rotation and magnetic field through porous medium on peristaltic transport of a Jeffrey fluid in tube. *Mathematical Problems in Engineering*, *2011*(1), 971456.

Moeana, F. K., & Al-Khafajy, D. G. S. (2024). Analyze a temperature and MHD peristaltic flow of sutterby fluid through a porous wavechannel in a rotating frame. *Journal of Al-Qadisiyah for Computer Science and Mathematics*, *16*(1), Page 34-49.

Mohammed, A. A., & Hummady, L. Z. (2023). Influence of heat transform and rotation of sutterby fluid in an asymmetric channel. *Iraqi Journal of Science*, 5766-5777.

Mustafa, M., Hayat, T., & Alsaedi, A. (2017). Rotating flow of Maxwell fluid with variable thermal conductivity: an application to non-Fourier heat flux theory. *International Journal of Heat and Mass Transfer*, *106*, 142-148.

Nadeem, S., & Akbar, N. S. (2009). Influence of heat transfer on a peristaltic transport of Herschel–Bulkley fluid in a non-uniform inclined tube. *Communications in Nonlinear Science and Numerical Simulation*, *14*(12), 4100-4113.

Nadeem, S., Akhtar, S., Akkurt, N., Saleem, A., Almutairi, S., & Ghazwani, H. A. (2023). Physiological peristaltic flow of Jeffrey fluid inside an elliptic cross section with heat and mass transfer: Exact solutions through Polynomial solution technique. *ZAMM-Journal of Applied Mathematics and Mechanics/Zeitschrift für Angewandte Mathematik und Mechanik*, *103*(3), e202100383.

Nadeem, S., & Akram, S. (2010). Peristaltic flow of a Williamson fluid in an asymmetric channel. *Communications in Nonlinear Science and Numerical Simulation*, *15*(7), 1705-1716.

Nadeem, S., Akram, S., Hayat, T., & Hendi, A. A. (2012). Peristaltic flow of a Carreau fluid in a rectangular duct.

Nallapu, S., & Radhakrishnamacharya, G. (2014). Jeffrey fluid flow through porous medium in the presence of magnetic field in narrow tubes. *International Journal of Engineering Mathematics*, *2014*(1), 713831.

Nallapu, S., & Radhakrishnamacharya, G. (2015). Jeffrey fluid flow through a narrow tubes in the presence of a magnetic field. *Procedia Engineering*, *127*, 185-192.

Nouri, J., & Whitelaw, J. (1997). Flow of Newtonian and non-Newtonian fluids in an eccentric annulus with rotation of the inner cylinder. *International Journal of Heat and Fluid Flow*, *18*(2), 236-246.

Pandey, S., & Tripathi, D. (2010). Unsteady model of transportation of Jeffrey-fluid by peristalsis. *International Journal of Biomathematics*, *3*(04), 473-491.

Rafiq, M., Sajid, M., Alhazmi, S. E., Khan, M. I., & El-Zahar, E. R. (2022). MHD electroosmotic peristaltic flow of Jeffrey nanofluid with slip conditions and chemical reaction. *Alexandria Engineering Journal*, *61*(12), 9977-9992.

Raptis, A., Perdikis, C., & Takhar, H. S. (2004). Effect of thermal radiation on MHD flow. *Applied Mathematics and Computation*, *153*(3), 645-649.

Reddy, M. G., & Reddy, K. V. (2015). Influence of Joule heating on MHD peristaltic flow of a nanofluid with compliant walls. *Procedia Engineering*, *127*, 1002-1009.

Salih, D. (2020). Influence of Varying Temperature and Concentration on (MHD) Peristaltic Transport for Jeffrey Fluid through an Inclined Porous Channel. *Journal of Physics: Conference Series*, *1664*, 012030. https://doi.org/10.1088/1742-6596/1664/1/012030

Scheidegger, A. E. (1957). *The physics of flow through porous media*. University of Toronto press.

Shaheen, A. (2017). *Peristaltic Flow of Newtonian and Non-Newtonian Fluids* CAPITAL UNIVERSITY OF SCIENCE & TECHNOLOGY ISLAMABAD].

Shaughnessy, E. J., Katz, I. M., & Schaffer, J. P. (2005). *Introduction to fluid mechanics* (Vol. 8). Oxford University Press New York.

Shruti, B., Alam, M. M., Parkash, A., & Dhinakaran, S. (2023). Darcy number influence on natural convection around porous cylinders in an enclosure using Darcy-Brinkman-Forchheimer model: LBM study. *Case Studies in Thermal Engineering*, *45*, 102907.

Sochi, T. (2010). Non-Newtonian flow in porous media. *Polymer*, *51*(22), 5007-5023.

Srinivas, S., & Kothandapani, M. (2009). The influence of heat and mass transfer on MHD peristaltic flow through a porous space with compliant walls. *Applied Mathematics and Computation*, *213*(1), 197-208.

Vaidya, H., Rajashekhar, C., Divya, B., Manjunatha, G., Prasad, K., & Animasaun, I. (2020). Influence of transport properties on the peristaltic MHD Jeffrey fluid flow through a porous asymmetric tapered channel. *Results in physics*, *18*, 103295.

Vajravelu, K., Sreenadh, S., & Lakshminarayana, P. (2011). The influence of heat transfer on peristaltic transport of a Jeffrey fluid in a vertical porous stratum. *Communications in Nonlinear Science and Numerical Simulation*, *16*(8), 3107-3125.

Vasudev, C., Rao, U. R., Rao, G. P., & Subba, M. (2011). Peristaltic flow of a Newtonian fluid through a porous medium in a vertical tube under the effect of a magnetic field. *Int J Cur Sci Res*, *1*(3), 105-110.